β-defensin genes were obtained. We used the basic local alignment search tool against the expressed sequence tag (EST) database and obtained a sequence identical with the DEFB6 gene (31). Based on this EST sequence (AW103145, AI910580) and the corresponding genomic sequence, we designed a pair of specific intron-spanning primers for RT-PCR (forward primer, 5′-CAGTCATGAGGACTTTCCTC-3′; reverse primer, 5′-AGA AGCTAGGTTATGTATGC-3′). Reverse transcription was performed on total human epididymis/testis RNA (Clontech Laboratories, Palo Alto, CA) using Superscript II. The PCR conditions were 94°C for 40 s, 60°C for 30 s, and 72°C for 1 min conducted for 35 cycles.

In addition, we designed two specific primers for RT-PCR based on the genomic sequence of the DEFB5 gene (forward primer, 5′-GTCGTG CAAGCTTGGTCGGG-3′; reverse primer, 5′-CCAGGTCTGCTTCTA AGGCC-3′) (31). We performed RT-PCR to evaluate the expression of this gene as described above. Subsequently, we determined the 5′ end of this novel cDNA sequence using a 5′ RACE kit (Life Technologies, Rockville, MD) performed on total RNA from the human epididymis.

Cloning of the mouse homologs of hBD-5, hBD-6, and HE2β1

We screened the homologous sequence of the DEFB5 gene using the basic local alignment search tool at NCBI and obtained the published full-length cDNA sequence from the adult mouse epididymis (AK020311, RIKEN full-length enriched library; clone 9230103N16) (32).

To identify the homolog of HE2β1, we designed a pair of degenerate PCR primers from the amino acid sequences conserved between HE2β1 and Bin1b: forward primer, 5′-GAYRTACCACCKGGAATHAG-3′; reverse primer, 5′-GATACRCARCATCTRTTCCA-3′. RT-PCR was performed on adult mouse epididymis RNA. The PCR conditions were 94°C for 40 s, 60°C for 30 s, and 72°C for 1 min conducted for 35 cycles. The sequencing of the PCR products revealed the homologous fragment with Bin1b cDNA. We screened the EST library using this novel nucleotide sequence and obtained the full-length cDNA sequence (AK020333, RIKEN full-length enriched library; clone 9230111C08) (32).

We also obtained the partial mouse genomic sequence containing the mBD-35 gene from the NCBI database (AL590619). This sequence was translated in all six possible reading frames and detected the homologous genomic sequence with the hBD-6 gene. Based on this genomic sequence, we designed two specific intron-spanning primers to confirm the expression (forward primer, 5′-GCCCTTCAGGTCATGAAGAC-3′; reverse primer, 5′-AGCATCTGCTTCCATCAGGT-3′). RT-PCR was performed as described on the DEFB6 gene. To determine the full-length cDNA sequences of these three mBD isoforms, we used 5′-RACE and 3′-RACE kits on the mouse epididymis RNA (Life Technologies).

Analysis of the genomic organization

As for human genomic sequences and mBD-11 genomic sequences, we used the public sequences at NCBI. As for the mBD-12 and mEP2e genomic sequences, we designed a pair of specific PCR primers from mBD-12 (forward primer, 5′-TGAAGAATCTCCCCTCAAACATGG-3′; reverse primer, 5′-TTCACAAGGCAAAGTTACAG-3′) and mEP2e (forward primer, 5′-ATCAGTCACACCTGCTTTCC-3′; reverse primer, 5′-ATCCTTTCACCGGACCTTTG-3′). PCR was performed on the isolated mouse genomic DNA using the Advantage HF-2 PCR kit (Clontech Laboratories). The PCR products were cloned to pCR4-TOPO vector (Invitrogen, Carlsbad, CA) and the inserts were sequenced to determine the splicing site.

Synthesis of mBD-12 mature peptide

We synthesized chemically the putative mBD-12 mature peptide spanning 34 COOH-terminal amino acids of the precursor at the Peptide Institute (Minoh, Japan). The synthetic peptide was air-oxidized for three disulfide bonds. The material, eluted in a single peak on RP-HPLC and confirmed by mass spectroscopy, was lyophilized and dissolved in 0.01% acetic acid.

Analysis of antimicrobial activity

We followed the colony count assay described by Harwig et al. (33) with some modification. Mid-logarithmic-phase *Escherichia coli* (ATCC 25922 strain) was suspended in 10 mM sodium phosphate buffer to adjust the density to 5×10^7 CFU/ml, and this suspension was mixed with mBD-12 solution. The final sodium concentration of this mixture was 15 mM, and the mBD-12 concentration was adjusted to 2, 20, or 200 μg/ml. As a control, the mixture without mBD-12 was also incubated. After a 2-h incubation of these mixtures at 37°C, the 10-fold serial dilutions were spread over tripticase soy agar plates and incubated at 37°C for 48 h. After counting the numbers of colonies on the plates, we calculated ratios of survived-to-control colony numbers as survival ratios.

The salt sensitivity of the antimicrobial activity was also evaluated. We adjusted the final sodium concentration of the bacterial mixture to 15, 50, 100, or 150 mM with NaCl and incubated the mixture for 2 h with 20 μg/ml mBD-12. As a control, the mixture without mBD-12 was also incubated at each sodium concentration. After the 2-h incubation, the 10-fold serial dilutions were spread over the plates and incubated for 48 h as described above. The procedures were repeated more than four times at each sodium concentration.

RT-PCR

Human epididymis and testis were obtained from the surgical samples of a prostate cancer patient in Mitsui Memorial Hospital (Tokyo, Japan). The institutional review board of Mitsui Memorial Hospital approved this study. We isolated human RNA from these specimens using Isogen (Nippon Gene, Toyama, Japan). We also purchased human RNA of brain, liver, lung, trachea, kidney, heart, and skeletal muscle from Clontech Laboratories. Mouse RNA was isolated from the indicated organs of sexually mature male ICR mice using Isogen (Nippon Gene). A total of 5 μg of each sample was reverse-transcribed by random hexamer primers using Superscript II (Life Technologies).

We designed a pair of specific intron-spanning primers from hBD-5 (forward primer, 5′-TTGGTTCAACTGCCATCAGG-3′; reverse primer, 5′-CCAGGTCTGCTTCTAAGGCC-3′), hBD-4 (forward primer, 5′-CTC CGACTTGCGTCTGCTTC-3′; reverse primer, 5′-CCTGAGCAAAACTT TCGATC-3′), and HE2β1 (forward primer, 5′-TCTGGCTTGCAGT GCTCTTG-3′; reverse primer, 5′-CTTGGGATACTTCAACATCC-3′). As other genes, we also designed a pair of specific intron-spanning primers from mBD-12 (forward primer, 5′-TGAAGAATCTCCCCT CAAACATGG-3′; reverse primer, 5′-GGAGCATAGCACTTTCGTTTG-3′), mEP2e (forward primer, 5′-ATCAGTCACACCTGCTTTCC-3′; reverse primer, 5′-CACATACTCAAAGCCTTTGG-3′), and mBD-3 (forward primer, 5′-GCTTCAGTCATGAGGATCCATTACCTTC-3′; reverse primer, 5′-GCTAGGGAGCACTTGTTTGCATTTAATC-3′). PCR was performed on 0.5 μl of reverse transcriptase reaction for a total volume of 25 μl using *Taq* polymerase (Takara Shuzo, Otsu, Japan). The PCR conditions were 94°C for 40 s, 60°C for 30 s, and 72°C for 1 min conducted for the indicated cycles. Amplification of G3PDH was also performed in parallel as a control.

In situ hybridization

A 290-bp fragment of mBD-11 cDNA, a 700-bp fragment of mBD-12 cDNA, and a 340-bp fragment of mEP2e cDNA were isolated from the mouse epididymis RNA as described above. We also isolated a 300-bp fragment containing mBD-3 exon 2 from bacterial artificial chromosome D11 (Incyte Genomics, Palo Alto, CA) by PCR amplification. Antisense and sense RNA probes were prepared from these fragments by T3 or T7 RNA polymerase using a DIG RNA labeling kit (Roche, Basel, Switzerland).

The mouse epididymis was fixed in 4% paraformaldehyde at 4°C overnight and was cryosectioned at 20 μm. The sections were treated with 1 μg/ml proteinase K for 5 min at 37°C and 2 mg/ml glycine for 30 s, postfixed in 3.7% formaldehyde in PBS for 20 min, and acetylated with 0.25% acetic anhydride in 0.1 M triethanolamine for 10 min. Hybridization with DIG-labeled probe was conducted overnight at 55°C in 5× SSC, 1% SDS, 50% formamide, and 1 mg/ml yeast tRNA containing 1 mg/ml probe. Then, the sections were washed twice in 2× SSC, 1% SDS, 50% formamide and once in 0.2× SSC, 0.1% SDS, 50% formamide at 60°C for 30 min each. The sections were incubated with anti-DIG alkaline phosphatase-conjugated Abs diluted 1/2000 with 100 mM maleic acid (pH 7.5), 50 mM NaCl, 0.1% Tween 20 overnight at 4°C, followed by an alkaline phosphatase reaction step under the following conditions: 50 mg/ml nitroblue tetrazolium chloride, 50 mg/ml 5-bromo-4-chloro-3-indolyl phosphate, 10% (w/v) polyvinylalcohol, 100 mM Tris-Cl (pH 9.5), 50 mM $MgCl_2$, 100 mM NaCl, 0.1% Tween 20. The sections were developed at 37°C in the dark.

Results
Identification of two novel hBD genes

Based on the public human genomic sequence (NT_019483), we identified multiple sequences that could be encoding β-defensin peptide because of its predicted cysteine pattern. We confirmed the existence of two corresponding transcripts of these putative genes by RT-PCR. The predicted amino acid sequences of these novel transcripts contained the specific six-cysteine motif identical with hBD-4 and we named these novel peptides hBD-5 and hBD-6, although the
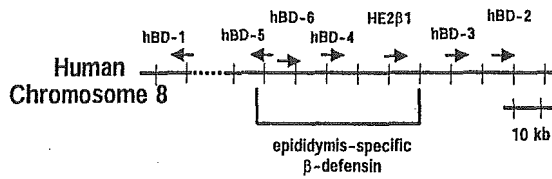
FIGURE 1. Schematic view of the hBD gene cluster on chromosome 8. The arrows indicate the direction of transcription of the indicated β-defensin isoforms. The epididymis-specific genes were located in the adjacent regions.

transcription initiation site of hBD-6 cDNA has not been determined, probably due to a too-low amount of hBD-6 mRNA.

The hBD-5 gene was located ~74.4 kb from the hBD-2 gene and ~19 kb from the hBD-4 gene (Fig. 1). The hBD-5 gene encoded its transcript in the antisense direction to the hBD-2, -3, -4, and HE2β1 genes. The hBD-6 gene was located between the hBD-4 and hBD-5 genes. hBD-5 contained three exons separated by the first 343-bp intron and the second 1248-bp intron while hBD-6 contained two exons separated by a 3575-bp intron (Fig. 2). No NF-κB consensus sites were found within the 5-kb promoter of the hBD-5 gene. The hBD-6 gene contains the NF-κB consensus sequence (GGGRNTYC) 5 and 1.3 kbp upstream of the

start codon like the hBD-2 gene, which contains multiple NF-κB binding sites (29, 34).

Identification of the mouse homolog of hBD-5, hBD-6, and HE2β1

RIKEN's full-length cDNA sequence from the adult mouse epididymis (AK020311) exhibited ~77% identity with the hBD-5 coding region. We also confirmed the transcript using RT-PCR, 5'-RACE, and 3'-RACE on the mouse epididymis RNA. Our sequence analysis contained a 2-nt difference from RIKEN's sequence in the 3' noncoding region. Because this mouse homolog corresponded to the Defb12 genomic sequence indicated by Schutte et al. (31), we named this isoform mBD-12. The genomic sequencing revealed that the mBD-12 gene was also separated by one short intron and one relatively long intron like hBD-5. The nucleotide sequence of the mBD-12 exon 3 coding region was 97.4% identical (191 of 196) with the corresponding sequence of mBD-35 cDNA (AJ437650) in the NCBI database, although mBD-12 exon 1 and exon 2 showed no homology with mBD-35. The genomic sequence of the second mBD-12 intron was also quite different from the mBD-35 genomic sequence, indicating that different genes encode these transcripts.
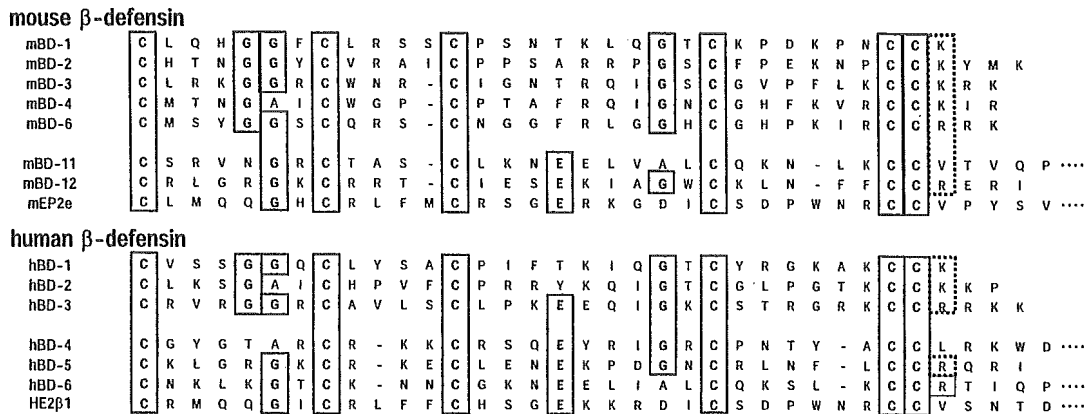
FIGURE 2. Nucleotide and amino acid sequences of hBD-5 (A) and hBD-6 (B). Exon sequences are shown in capital letters. The exon-intron splice site sequences conform to the consensus rule. The dashed underlining indicates a TATA box-like sequence of the hBD-5 promoter. The boxes indicate the specific cysteine residues identical with hBD-4 and the dashed boxes indicate the additional cysteine residues unique to hBD-5, hBD-6, and their mouse homologs.

mouse β-defensin

```
mBD-1   C L Q H G G F C L R S S C P S N T K L Q G T C K P D K P N C C K
mBD-2   C H T N G G Y C V R A I C P P S A R R P G S C F P E K N P C C K Y M K
mBD-3   C L R K G G R C W N R - C I G N T R Q I G S C G V P F L K C C K R K
mBD-4   C M T N G A I C W G P - C P T A F R Q I G N C G H F K V R C C K I R
mBD-6   C M S Y G G S C Q R S - C N G G F R L G G H C G H P K I R C C R R K

mBD-11  C S R V N G R C T A S - C L K N E E L V A L C Q K N - L K C C V T V Q P ....
mBD-12  C R L G R G K C R R T - C I E S E K I A G W C K L N - F F C C R E R I
mEP2e   C L M Q Q G H C R L F M C R S G E R K G D I C S D P W N R C C V P Y S V ....
```

human β-defensin

```
hBD-1   C V S S G G Q C L Y S A C P I F T K I Q G T C Y R G K A K C C K
hBD-2   C L K S G A I C H P V F C P R R Y K Q I G T C G L P G T K C C K K P
hBD-3   C R V R G G R C A V L S C L P K E E Q I G K C S T R G R K C C R R K K

hBD-4   C G Y G T A R C R - K K C R S Q E Y R I G R C P N T Y - A C C L R K W D ....
hBD-5   C K L G R G K C R - K E C L E N E K P D G N C R L N F - L C C R Q R I
hBD-6   C N K L K G T C K - N N C G K N E E L I A L C Q K S L - K C C R T I Q P ....
HE2β1   C R M Q Q G I C R L F F C H S G E K K R D I C S D P W N R C C V S N T D ....
```

FIGURE 3. Comparison of the predicted amino acid sequences of the hBD and mBD families. Shown are partial amino acid sequences of the hBD and mBD isoforms whose tissue distribution was evaluated. The isoforms below the space were included in the epididymis-specific β-defensin subgroup. The solid boxes indicate the conserved residues among the multiple hBDs and mBDs. The dashed boxes show the conserved cationic residues.

Degenerate PCR amplification of the mouse epididymis cDNA with primers common to HE2β1 and Bin1b revealed a novel β-defensin sequence homologous with Bin1b. The cDNA sequence was identical with RIKEN's full-length cDNA sequence of the adult mouse epididymis (AK020333) (32). We also confirmed the corresponding transcript using RT-PCR, 5'-RACE, and 3'-RACE on the mouse epididymis RNA. The predicted amino acid sequence of this cDNA is 68.1% (47 of 69) identical with chimpanzee EP2E and 88.4% (61 of 69) identical with Bin1b, and we named this β-defensin isoform mEP2e. The genomic sequence revealed that the mEP2e gene was composed of only two exons separated by an ~1.2-kb intron, supporting mEP2e correspond to the EP2E splicing variant in the chimpanzee EP2 gene. The HE2β1 gene was composed of three exons separated by the first 583-bp intron and the second 11815-bp intron corresponding to the EP2D isoform (9–11, 28). The amino acid sequence encoded by the mEP2e exon 2 was also 67.3% (35 of 52) identical with the corresponding sequence of HE2β1. We could not detect the mouse variant corresponding to the EP2D isoform using the 5'-RACE system.

Using the public mouse nucleotide database at the NCBI (AL580619), we detected the genomic sequence homologous with the hBD-6 gene and confirmed the corresponding transcript using RT-PCR, 5'-RACE, and 3'-RACE on the mouse epididymis RNA. This mouse homolog was completely identical with defb11 gene at the NCBI database (AJ437648), named mBD-11. The predicted amino acid sequence of mBD-11 is 70.9% (46 of 65) identical with hBD-6 corresponding sequence. mBD-11 was composed of two exons separated by a 2567-bp intron like hBD-6. No NF-κB consensus sites were found within the 5-kb promoter of the mBD-12 gene.

Comparison of the hBD and mBD isoforms

In Fig. 3, we compared the partial amino acid sequences of hBD-5, hBD-6, mBD-11, mBD-12, and mEP2e with the known β-defensin isoforms whose tissue distribution had been evaluated. All the isoforms contain the specific cysteine motif (whose cysteine residues are referred to as C1, C2, C3, C4, C5, and C6 residues in order here).

Although the amino acid sequences were quite variable among the members of the β-defensin family, except the specific cysteine motif, there are some residues relatively conserved, such as the glycine two positions before the C2 residue (Fig. 3). As described below, mBD-11, mBD-12, and mEP2e in the mBD family and HE2β1, hBD-4, hBD-5, and hBD-6 in the hBD family showed the epididymis-specific expression pattern. These isoforms conserve

the glutamic acid residue six positions before the C4 residue and do not conserve the glycine residue three positions before the C2 residue. These features are rather common among the potentially new β-defensin isoforms whose expression had not been established (33). Interestingly, α-defensin also includes the glutamic acid residue six positions before the C4 residue (1, 35).

Antimicrobial activity of synthetic mBD-12 peptide

To confirm the antimicrobial activity of mBD-12, we synthesized a putative mature peptide of mBD-12. The synthetic peptide

A

B
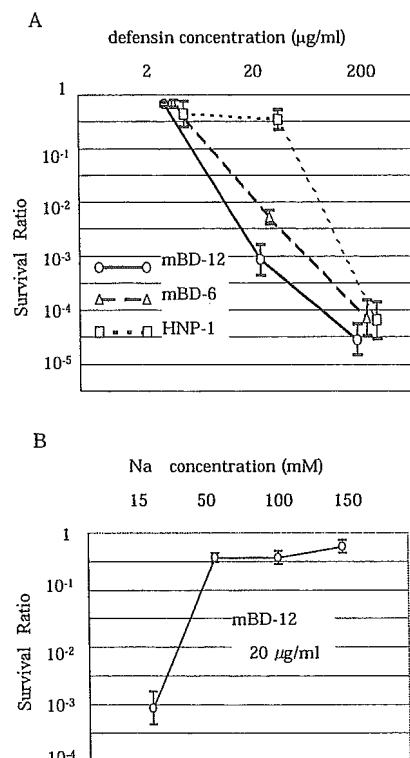
FIGURE 4. Antimicrobial activity of mBD-12 synthetic peptide. The survival ratio is the ratio of the number of survived colonies to that of control colonies. The means and the SEs of the $\log_{10}$ survival ratio are depicted. We also added the data of mBD-6 and HNP-1, which had been previously reported. A, mBD-12 showed significantly more potent microbicidal activity against E. coli at the concentration of 20 μg/ml than HNP-1 (Student's t test, $p < 0.01$). B, mBD-12 antimicrobial activity was significantly reduced at the environmental sodium concentrations of 50, 100, and 150 mM (Student's t test, $p < 0.01$).

showed bactericidal activity against *E. coli*. We compared the potency of mBD-12 with mBD-6 and HNP-1 synthetic peptide, whose data had been previously reported (20). mBD-12 bactericidal activity was significantly more potent than HNP-1 at the concentration of 20 μg/ml (Student's t test, $p < 0.01$) (Fig. 4A). This potency was comparable to other β-defensins because the minimum inhibitory concentration of recombinant mBD-3 was 16 μg/ml against *E. coli* and the effective concentration of hBDs ranged from 5 to 60 μg/ml (5–7, 13, 14). The antimicrobial potency of mBD-12 was significantly reduced at high concentrations of NaCl like hBD1, hBD-2, hBD-4, mBD-1, and mBD-6 (Student's t test, $p < 0.01$) (Fig. 4B) (5, 7, 13, 14).

Tissue distribution of hBD-5, hBD-6, mBD-11, mBD-12, and mEP2e

RT-PCR revealed that hBD-5 and hBD-6 were specifically expressed in the human epididymis (Fig. 5A). No signal was detected in the other main organs: brain, trachea, lung, heart, liver, kidney, skeletal muscle, and testis. This expression pattern was similar to that of hBD-4. Although a previous report has shown the main expression of hBD-4 in the testis, our data more precisely indicate the hBD-4 expression in the human epididymis but not in the testis (7). HE2β1 expression has never been evaluated well. Our RT-PCR amplification of human epididymis RNA revealed a 546-bp fragment consistent with HE2α1 and a 470-bp fragment consistent with HE2β1, confirmed by sequencing. Although weak signals

were also detected in the trachea or lung, the specific amplification of HE2 family was not confirmed by sequencing in this tissue, indicating that HE2 expression would be also confined to the epididymis.

To evaluate the mBD-11, mBD-12, and mEP2e expression, we isolated total RNA from the intestine, stomach, liver, kidney, heart, brain, esophagus, tongue, lung, trachea, skeletal muscle, epididymis, and testis of a male ICR mouse aged 4 mo. RT-PCR of mBD-11, mBD-12, and mEP2e also revealed the epididymis-specific tissue distribution (Fig. 5B). The tissue specificity of these isoforms was clearly different from mBD-3. RT-PCR revealed mBD-3 expression in the mouse esophagus and tongue, consistent with previous reports (18–20). Interestingly, we also detected weak mBD-3 expression in the mouse epididymis, which had not been evaluated well (18). The mBD-3 expression in the epididymis was demonstrated more clearly in Fig. 6 using the 35-cycle PCR. RT-PCR analysis of mBD-1, mBD-2, and mBD-6 also showed their expression in the mouse epididymis, whereas mBD-4 expression was not detected (data not shown).

PCR amplification of mBD-12 revealed one larger 700-bp fragment and one shorter 385-bp fragment using the specific primers from the exon 1 and the 3' noncoding region. Sequencing of the PCR products indicated the larger one corresponding to mBD-12
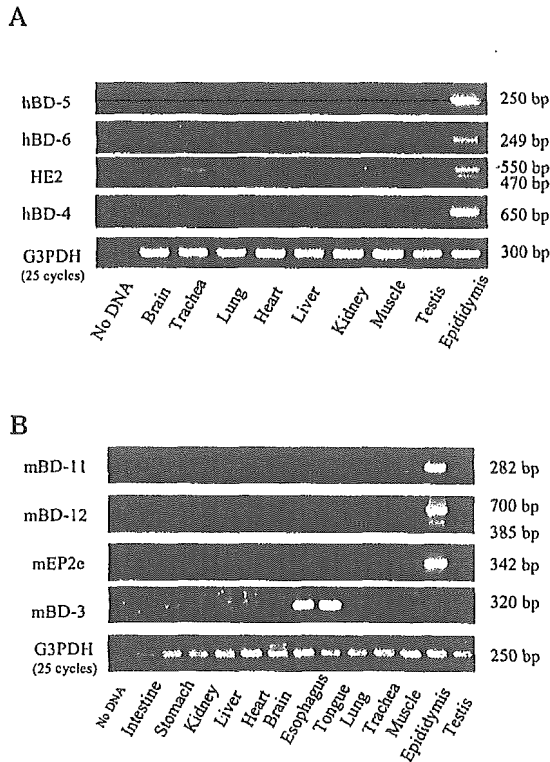
FIGURE 5. Tissue distribution of novel β-defensin isoforms in humans (*A*) and mice (*B*). RT-PCR of the indicated β-defensin isoforms and G3PDH was performed from the total RNA of the indicated tissues in humans or mice. PCR of β-defensin cDNA was conducted for 30 cycles and PCR of G3PDH was conducted for 25 cycles. hBD-4, hBD-5, hBD-6, HE2β1, and their mouse homologs are all predominantly expressed in the epididymis. The amplification of HE2 cDNA revealed a 546-bp fragment, consistent with HE2α1, and a 470-bp fragment, consistent with HE2β1. The amplification of mBD-12 also revealed a weak 385-bp fragment corresponding to the alternative spliced product. mBD-3 expression was detected in the esophagus, tongue, stomach, and epididymis.
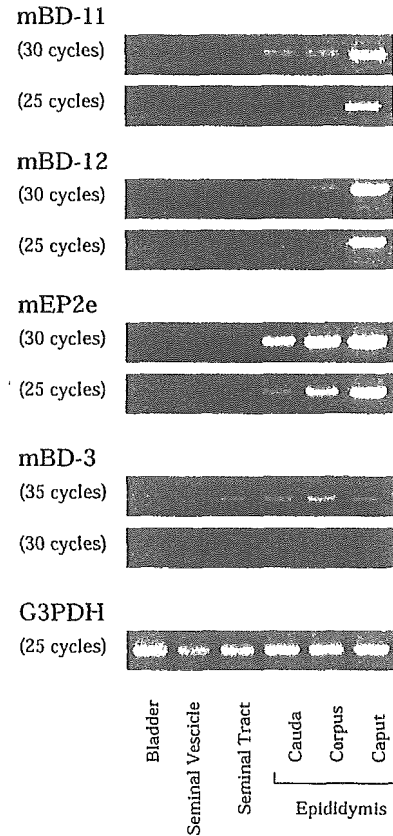
FIGURE 6. RT-PCR analysis of the regional specificity of the mBD family in the epididymis. We isolated total RNA from the mouse bladder, seminal vesicle, seminal duct, and the epididymis caput, corpus, and caudal region separately. RT-PCR detected mBD-11 and mBD-12 expression most prominent in the epididymis caput region especially after 25 cycles, and completely absent in the seminal tract, seminal vesicle, and bladder. mEP2e expression was also most prominent in the caput region, but the compatible expression was also detected in the corpus region even after 25 cycles. RT-PCR of mBD-3 showed ubiquitous expression in the caput region, corpus region, and caudal region. mBD-3 expression was detected even in the seminal tract.

and the shorter one corresponding to the novel transcripts that contained the identical sequences with the 5' end of mBD-12 exon 1 and the 3' noncoding region of mBD-12 exon 3, suggesting that they were alternatively spliced exons encoded by a single gene.

Region specificity of mBD-11, mBD-12, and mEP2e expression in the mouse epididymis

Our evaluation of tissue distribution suggested the importance of the β-defensin family in the male reproductive organ. To further investigate the precise distribution of their expression, we isolated total RNA from the caput, corpus, and caudal region of the adult mouse epididymis separately. We also isolated total RNA from the mouse seminal duct, seminal vesicle, and bladder. RT-PCR revealed that mBD-11 and mBD-12 expression was most prominent in the epididymis caput region and was completely absent in the seminal tract, seminal vesicle, and bladder (Fig. 6). mEP2e expression was also most prominent in the caput region, but the compatible expression was also detected in the corpus region. RT-PCR of mBD-3 showed ubiquitous expression in the caput, corpus, and caudal region and even in the seminal tract. mBD-1, mBD-2,
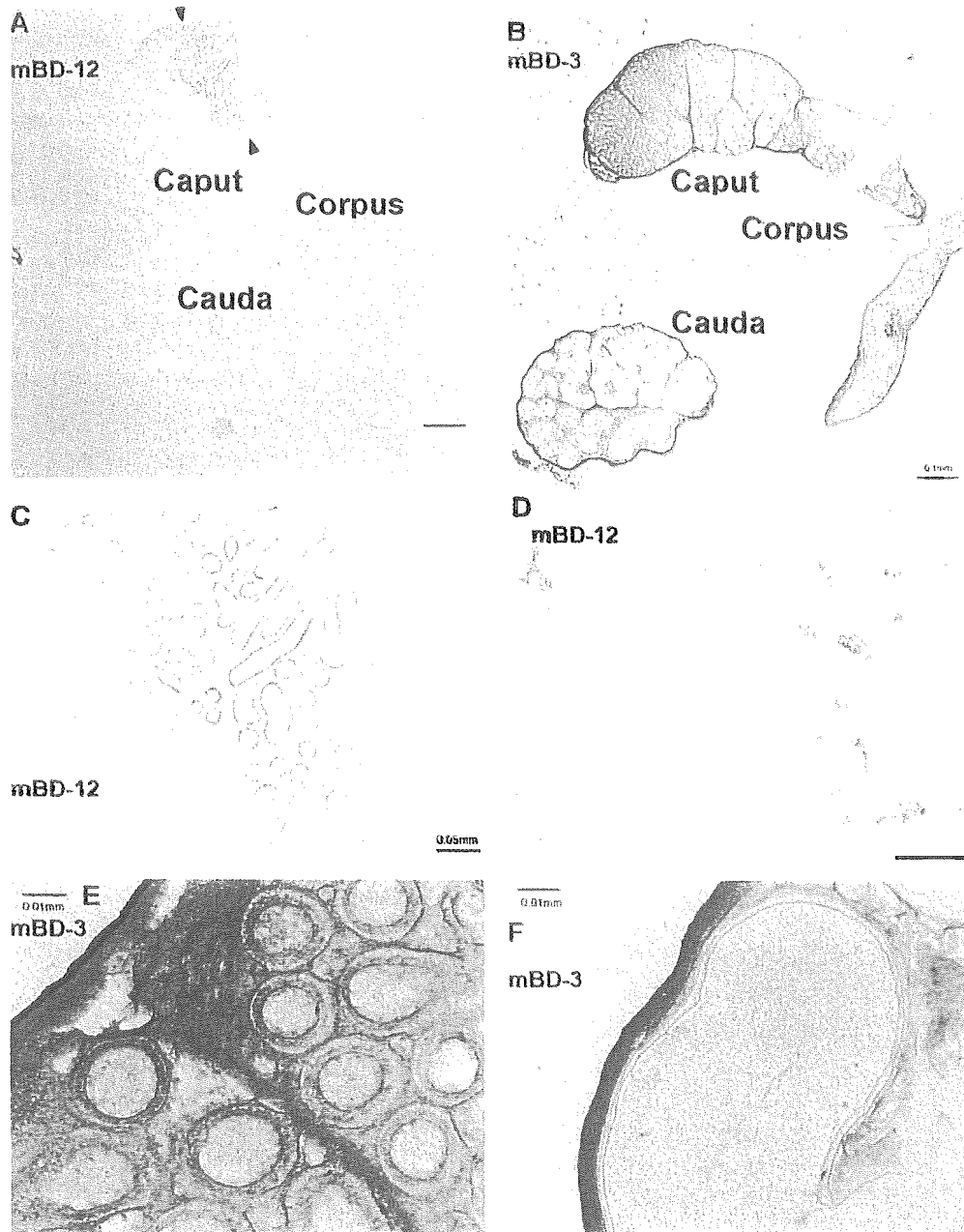
FIGURE 7. In situ hybridization of the epididymis with mBD-12 and mBD-3 antisense probe. The cryosectioned epididymis slides were hybridized with the indicated antisense probe. *A*, Low magnification. The hybridization signals of the mBD-12 antisense probe were confined to the epithelial cells of the epididymis caput mid/distal segment indicated by the arrows. No signals were detected in the corpus or caudal region. *B*, Low magnification. The hybridization signals of the mBD-3 antisense probe were present in the capsule and septum of the whole epididymis. *C*, The higher magnification of the caput region revealed more clearly the confined distribution of mBD-12 mRNA. *D*, The higher magnification of the box in Fig. 8*B* indicated the mBD-12 regulation at the cellular level. Some epithelial cells exhibited strong signals, whereas adjacent epithelial cells exhibited none, indicating the cell specificity of its expression. *E* and *F*, The higher magnification of the caput region (*E*) and caudal region (*F*) also revealed more clearly mBD-3 expression in the mesenchymal cells surrounding and compartmentalizing the epididymis. The lower signals were also present in the connective tissues around the epithelial cells. Scale bars = 100 (*A* and *B*), 50 (*C*), 25 (*D*), and 10 (*E* and *F*) μm.

and mBD-6 also showed the ubiquitous expression in the whole epididymis (data not shown).

To confirm the region-specific expression of mBD-11, mBD-12, and mEP2e in the mouse epididymis, we analyzed the distribution of mBD-11, mBD-12, mEP2e, and mBD-3 mRNA at the cellular level using in situ hybridization. The hybridization signals of the mBD-11, mBD-12, or mEP2e antisense probe were confined to the epithelial cells of the mid/distal segment of the caput region, indicating the region specificity of their expression (Figs. 7 and 8). Higher magnification also revealed more complex regulation of mBD-12 or mEP2e expression; i.e., some epithelial cells exhibited strong signals whereas the adjacent epithelial cells exhibited none in the same segment, indicating the cell specificity of their expression (Fig. 7D). The sense probes gave no hybridization signals (data not shown).

Parallel sections were hybridized to mBD-3 probes that gave distinct expression patterns. The most strong mBD-3 hybridization signals were present in the mesenchymal cells surrounding and compartmentalizing the epididymis, while lower signals were present in the connective tissues around the epithelial cells. This expression pattern was conserved in the caput, corpus, and caudal region, consistent with our data of RT-PCR (Fig. 7).

We compared the region specificity among mBD-11, mBD-12, and mEP2e by hybridization of adjacent sections with each probe. Their signals were almost colocalized in the mid/distal segment of the caput region (Fig. 8). However, a narrow portion adjacent to the initial segment exhibited mBD-12 hybridization signals more intensely and a relatively wide distal portion exhibited mEP2e hy-

A mBD-11

B mBD-12

C mEP2e

FIGURE 8. In situ hybridization of mBD-11, mBD-12, and mEP2e mRNA in the epididymis. The parallel section was hybridized with mBD-11 (A), mBD-12 (B), or mEP2e (C) antisense probe. Because B and C are adjacent sections, the region specificity of mBD-12 and mEP2e expression can be precisely evaluated. A, mBD-11 signals were confined to the mid/distal segment of the caput region. B, mBD-12 signals were also confined to the mid/distal segment of the caput region. The distal region shown by the arrowheads exhibited no mBD-12 signals, although mEP2e signals were intense in this region, shown in C. The higher magnification of the box was shown in Fig. 7D. C, mEP2e signals were also confined to the mid/distal segment of the caput region. However, the narrow region shown by the arrowheads exhibited no mEP2e signals, although mBD-12 signals were intense in this region, shown in B. Scale bars = 100 μm.

bridization signals more intensely, consistent with the RT-PCR analysis.

Discussion

In this work we describe the identification of the epididymis-specific β-defensin isoforms including two novel hBD, termed hBD-5 and hBD-6, and the mouse homologs of hBD-5, hBD-6, and HE2β1, termed mBD-12, mBD-11, and mEP2e, respectively.
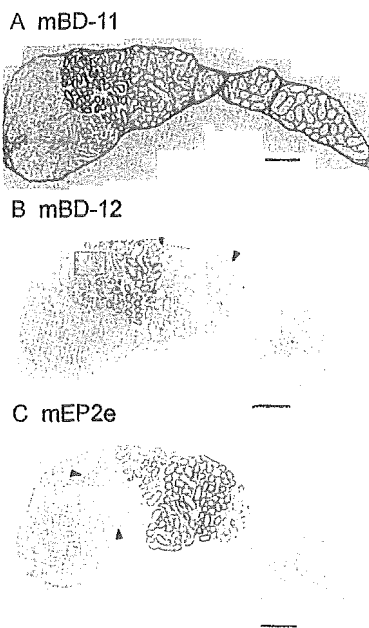
The organization of gene cluster is a peculiar feature of the defensin family and prompted us to use the human genomic sequence to search novel defensin genes. Because multiple isoforms of the β-defensin family had been identified in human and mouse organs and may compensate each other for their common functions in part, the overall identification of β-defensin isoforms is very important to study their physiological roles.

hBD-5, hBD-6, hBD-4, and HE2β1 were specifically expressed in the human epididymis. Because the epididymis is anatomically continuous to the urethra, it is always at the risk of ascending microbial invasion. Acute epididymitis is a common sexually transmitted disease, caused by bacterial infection of the epididymis. Therefore, host defense against a bacterial pathogen would be very important in the epididymis for the protection of spermatozoa.

Our identification of the novel mBD, mBD-12, and mEP2e would also be noteworthy because animal models are very useful to understand the physiological and pathological significance of these peptides. The comparison of the genomic organization of HE2β1 and mEP2e revealed that HE2β1 and mEP2e would be included in different message variants. Although the genomic sequence of the HE2 gene indicated the possible existence of another promoter within the second intron of the HE2β1 gene, no transcripts corresponding to the EP2e isoform have been identified in humans. Considering that no splicing variants corresponding to the HE2β1 isoform were detected in mice, the major transcript would be different between humans and mice, at least at a basal state.

Our identification of the epididymis-specific β-defensin isoforms clarified the existence of two groups in the β-defensin family: epididymis-specific isoforms and the other isoforms. The former includes HE2β1, hBD-4, hBD-5, and hBD-6 and the latter includes hBD-1, hBD-2, and hBD-3 in humans. Interestingly, the epididymis-specific β-defensin genes were located within a region encompassing ~40 kb in the human defensin gene cluster on chromosome 8. In mice, this report first indicated that mBD-11, mBD-12, and mEP2e are expressed, and that their expression is epididymis specific. Between the two groups, some different features are present in their amino acid sequences. First, the amino acid sequences of the epididymis-specific β-defensin isoforms were well conserved between humans and mice in comparison with the other β-defensin isoforms. Although mBD-3 had been regarded as a hBD-2 homolog, the amino acid sequence identity was only 40%. In contrast, mBD-11, mBD-12, and mEP2e were >65% identical with their human homologs. Second, some amino acid residues are different between the two groups. The glutamic acid residue is conserved in six positions before the C4 residue in the epididymis-specific β-defensin isoforms, and this feature is conserved even in the α-defensin family. Although few conserved residues have been indicated, except the cysteine motif, between the α-defensin and β-defensin families and it had been questioned whether the two families have really descended from a single ancestral gene, this common feature would support the evolutionary continuity between the α-defensin and β-defensin families (36). In addition, these features would reflect the existence of some specific microenvironmental condition of host defense in the epididymis.

Our evaluation of the mBD-11, mBD-12, mEP2e, and mBD-3 expression pattern in the epididymis revealed mBD-11, mBD-12,

and mEP2e expression in the epithelial cells of the mid/distal segment of the caput region and mBD-3 expression in the capsule and septum of the whole epididymis. These findings also clarify the different features between the epididymis-specific isoforms and the other β-defensin isoforms.

More interestingly, mBD-11, mBD-12, and mEP2e were expressed in different regions, although major portions of the middle segment expressed both genes. In general, the epididymis displays a highly region-specific and cell-specific pattern of gene expression (37, 38). This spatial regulation would make different luminal environments, and in these specific environments the specific functions of the epididymis would be conducted, such as regulation of sperm maturation, storage of mature spermatozoa, and protection from pathogens or reactive oxygen. Our results indicate that some different regional regulation would be also working among the members of the epididymis-specific β-defensin family, suggestive of their roles in the specific functions of the epididymis, although this issue remains to be investigated more clearly.

Acknowledgments

References

1. Ganz, T., M. E. Selsted, D. Szklarek, S. S. L. Harwig, K. Daher, D. F. Bainton, and R. I. Lehrer. 1985. Defensins: natural peptide antibiotics of human neutrophils. *J. Clin. Invest. 76:1427.*
2. Diamond, G., M. Zasloff, H. Eck, M. Brasseur, W. L. Maloy, and C. L. Bevins. 1991. Tracheal antimicrobial peptide, a cysteine-rich peptide from mammalian tracheal mucosa: peptide isolation and cloning of a cDNA. *Proc. Natl. Acad. Sci. USA 88:3952.*
3. Schonwetter, B. S., E. D. Stolzenberg, and M. A. Zasloff. 1995. Epithelial antibiotics induced at sites of inflammation. *Science 267:1645.*
4. Bensch, K. W., M. Raida, H. J. Magert, P. Schulz-Knappe, and W. G. Forssmann. 1995. hBD-1: a novel β-defensin from human plasma. *FEBS Lett. 368:331.*
5. Harder, J., J. Bartels, E. Christophers, and J. M. Schröder. 1997. A peptide antibiotic from human skin. *Nature 387:861.*
6. Harder, J., J. Bartels, E. Christophers, and J. M. Schröder. 2001. Isolation and characterization of human β-defensin-3, a novel human inducible peptide antibiotic. *J. Biol. Chem. 276:5707.*
7. Garcia, J. R., A. Krause, S. Schulz, F. J. Rodriguez-Jimenez, E. Kluver, K. Adermann, U. Forssmann, A. Frimpong-Boateng, R. Bals, and W. G. Forssmann. 2001. Human β-defensin 4: a novel inducible peptide with a specific salt-sensitive spectrum of antimicrobial activity. *FASEB J. 15:1819.*
8. Osterhoff, C., C. Kirchhoff, N. Krull, and R. Ivell. 1994. Molecular cloning and characterization of a novel human sperm antigen (HE2) specifically expressed in the proximal epididymis. *Biol. Reprod. 50:516.*
9. Hamil, K. G., P. Sivashanmugam, R. T. Richardson, G. Grossman, S. M. Ruben, J. L. Mohler, P. Petrusz, M. G. O'Rand, F. S. French, and S. H. Hall. 2000. HE2β and HE2γ, new members of an epididymis-specific family of androgen-regulated proteins in the human. *Endocrinology 141:1245.*
10. Fröhlich, O., C. Po, and L. G. Young. 2001. Organization of the human gene encoding the epididymis-specific EP2 protein variants and its relationship to defensin genes. *Biol. Reprod. 64:1072.*
11. Jia, H. P., B. C. Schutte, A. Schudy, R. Linzmeier, J. M. Guthmiller, G. K. Johnson, B. F. Tack, J. P. Mitros, A. Rosenthal, T. Ganz, and P. B. McCray, Jr. 2001. Discovery of new human β-defensins using a genomics-based approach. *Gene 263:211.*
12. Goldman, M. J., M. G. Anderson, E. D. Stolzenberg, P. U. Kari, M. Zasloff, and J. M. Wilson. 1997. Human β-defensin-1 is a salt-sensitive antibiotic in lung that is inactivated in cystic fibrosis. *Cell 88:553.*
13. Valore, E. V., C. H. Park, A. J. Quayle, K. R. Wiles, P. B. McCray, Jr., and T. Ganz. 1998. Human β-defensin-1: an antimicrobial peptide of urogenital tissues. *J. Clin. Invest. 101:1633.*
14. Bals, R., X. Wang, Z. Wu, T. Freeman, V. Bafna, M. Zasloff, and J. M. Wilson. 1998. Human β-defensin 2 is a salt-sensitive peptide antibiotic expressed in human lung. *J. Clin. Invest. 102:874.*
15. Huttner, K. M., C. A. Kozak, and C. L. Bevins. 1997. The mouse genome encodes a single homolog of the antimicrobial peptide human β-defensin 1. *FEBS Lett. 413:45.*
16. Bals, R., M. J. Godman, and J. M. Wilson. 1998. Mouse β-defensin 1 is a salt-sensitive antimicrobial peptide in epithelia of the lung and urogenital tract. *Infect. Immun. 66:1225.*
17. Morrison, G. M., D. J. Davidson, and J. R. Dorin. 1999. A novel mouse β defensin, Defb2, which is upregulated in the airways by lipopolysaccharide. *FEBS Lett. 442:112.*
18. Bals, R., X. Wang, R. L. Meegalla, S. Wattler, D. Weiner, M. C. Nehls, and J. M. Wilson. 1999. Mouse β-defensin 3 is an inducible antimicrobial peptide expressed in the epithelia of multiple organs. *Infect. Immun. 67:3542.*
19. Jia, H. P., S. A. Wowk, B. C. Schutte, S. K. Lee, A. Vivado, B. F. Tack, C. L. Bevins, and P. B. McCray, Jr. 2000. A novel murine β-defensin expressed in tongue, esophagus, and trachea. *J. Biol. Chem. 275:33314.*
20. Yamaguchi, Y., S. Fukuhara, T. Nagase, T. Tomita, S. Hitomi, S. Kimura, H. Kurihara, and Y. Ouchi. 2001. A novel mouse β-defensin, mBD-6, predominantly expressed in skeletal muscle. *J. Biol. Chem. 276:315.*
21. Bauer, F., K. Schweimer, E. Kluver, J. R. Conejo-Garcia, W. G. Forssmann, P. Rosch, K. Adermann, and H. Sticht. 2001. Structure determination of human and murine β-defensins reveals structural conservation in the absence of significant sequence similarity. *Protein Sci. 10:2470.*
22. Zhao, C., I. Wang, and R. L. Lehrer. 1996. Widespread expression of β-defensin hBD-1 in human secretory glands and epithelial cells. *FEBS Lett. 396:319.*
23. Fulton, C., G. M. Anderson, M. Zasloff, R. Bull, and A. G. Quinn. 1997. Expression of natural peptide antibiotics in human skin. *Lancet 350:1750.*
24. McCray, P. B., Jr., and L. Bentley. 1997. Human airway epithelia express a β-defensin. *Am. J. Respir. Cell Mol. Biol. 16:343.*
25. O'Neil, D. A., E. M. Porter, D. Elewaut, G. M. Anderson, L. Eckmann, T. Ganz, and M. F. Kagnoff. 1999. Expression and regulation of the human β-defensins hBD-1 and hBD-2 in intestinal epithelium. *J. Immunol. 163:6718.*
26. Garcia, J. R., F. Jaumann, S. Shulz, A. Krause, J. Rodriguez-Jimenez, U. Forssmann, K. Adermann, E. Kluver, C. Vogelmeier, D. Becker, et al. 2001. Identification of a novel, multifunctional β-defensin (human β-defensin 3) with specific antimicrobial activity: its interaction with plasma membranes of *Xenopus* oocytes and the induction of macrophage chemoattraction. *Cell Tissue Res. 306: 257.*
27. Li, P., H. C. Chan, B. He, S. C. So, Y. W. Chung, Q. Shan, Y. D. Zhang, and Y. L. Zhang. 2001. An antimicrobial peptide gene found in the male reproductive system of rats. *Science 291:1783.*
28. Fröhlich, O., C. Po, T. Murphy, and L. G. Young. 2000. Multiple promoter and splicing mRNA variants of the epididymis-specific gene EP2. *J. Androl. 21:421.*
29. Liu, L., L. Wang, H. P. Jia, C. Zhao, H. H. Q. Heng, B. C. Schutte, P. B. McCray, Jr., and T. Ganz. 1998. Structure and mapping of the human β-defensin HBD-2 gene and its expression at sites of inflammation. *Gene 222:237.*
30. Linzmeier, R., C. H. Ho, B. V. Hoang, and T. Ganz. 1999. A 450-kb contig of defensin genes on human chromosome 8p23. *Gene 233:205.*
31. Schutte, B. C., J. P. Mitros, J. A. Bartlett, J. D. Walters, H. P. Jia, M. J. Welsh, T. L. Casavant, and P. B. McCray, Jr. 2002. Discovery of five conserved β-defensin gene clusters using a computational search strategy. *Proc. Natl. Acad. Sci. USA 99:2129.*
32. Kawai, J., A. Shinagawa, K. Shibata, M. Yoshino, M. Itoh, Y. Ishii, T. Arakawa, A. Hara, Y. Fukunishi, H. Konno, et al. 2001. Functional annotation of a full-length mouse cDNA collection. *Nature 409:685.*
33. Harwig, S. S., T. Ganz, and R. I. Lehrer. 1994. Neutrophil defensins: purification, characterization, and antimicrobial testing. *Methods Enzymol. 236:160.*
34. Becker, M. N., G. Diamond, M. W. Verghese, and S. H. Randell. 2000. CD14-dependent lipopolysaccharide-induced β-defensin-2 expression in human tracheobronchial epithelium. *J. Biol. Chem. 275:29731.*
35. Lehrer, R. I., and T. Ganz. 1990. Antimicrobial polypeptides of human neutrophils. *Blood 76:2169.*
36. Hughes, A. L. 1999. Evolutionary diversification of the mammalian defensins. *Cell. Mol. Life Sci. 56:94.*
37. Rodriguez, C. M., J. L. Kirby, and B. T. Hinton. 2000. Regulation of gene transcription in the epididymis. *Reproduction 122:41.*
38. Orgebin-Crist, M. C. 1995. Androgens and epididymal function. In *Pharmacology, Biology, and Clinical Applications of Androgens.* D. Bhasin, H. L. Gabelnick, J. M. Spieler, R. S. Swerdloff, and C. Wang, eds. Wiley-Liss, New York, p. 27.

ORIGINAL ARTICLE

Molecular mechanisms underlying human β-defensin-2 gene expression in a human airway cell line (LC2/ad)

Tetsuji TOMITA, Takahide NAGASE, Eijiro OHGA, Yasuhiro YAMAGUCHI, Masao YOSHIZUMI AND Yasuyoshi OUCHI

Department of Geriatric Medicine, Graduate School of Medicine, University of Tokyo, Tokyo, Japan

Molecular mechanisms underlying human β-defensin-2 gene expression in a human airway cell line (LC2/ad)
TOMITA T, NAGASE T, OHGA E, YAMAGUCHI Y, YOSHIZUMI M, OUCHI Y. *Respirology* 2002; **7**: 305–310
Objective: Recently, human β-defensin-2 (hBD-2), an inducible defensin, has been reported to be involved in innate immunity and host defence. To examine the exact roles of hBD-2 in the respiratory system, we examined the molecular mechanisms of hBD-2 gene expression *in vitro*.
Methodology: Using a human airway cell line (LC-2/ad), lipopolysaccharide (LPS)-induced gene expression of hBD-2 was studied in the absence or the presence of (i) dexamethasone, (ii) inhibition of NF-κB and AP-1, (iii) intracellular calcium chelator, and (iv) cyclooxygenase (COX) inhibitors.
Results: Lipopolysaccharide-induced gene expression of hBD-2 was down-regulated by (i) dexamethasone, (ii) inhibition of NF-κB and AP-1, and (iii) intracellular calcium chelator. However, COX inhibitors had no effect on LPS-induced mRNA expression of hBD-2.
Conclusion: These findings suggest that glucocorticoids (GC), but not COX inhibitors, reduce hBD-2 gene expression, while NF-κB, AP-1 and intracellular calcium are essential for hBD-2 expression. Glucocorticoid-induced down-regulation of hBD-2 might be involved in the GC-induced suppression of respiratory host defence associated with hBD-2.

Key words: cyclooxygenase inhibitors, glucocorticoids, human β-defensin-2, intracellular calcium, NF-κB.

INTRODUCTION

Antimicrobial peptides including β-defensins are thought to be effective against opportunistic infections.[1,2] In humans, three β-defensins have been identified. The first human β-defensin, hBD-1, is predominantly expressed in epithelia of the urogenital tract and has been reported to be constitutive.[3–5] The second and third human β-defensins, hBD-2 and hBD-3, were isolated from psoriatic skin and found to be predominantly expressed in the skin and respiratory tract.[6,7] Of note, hBD-2 gene expression is inducible by various proinflammatory agents such as TNF-α, IL-1β, IL-8, lipopolysaccharide (LPS),

bacteria, and yeasts.[6,8–11] It has been shown that LPS-induced expression of hBD-2 in human tracheobronchial epithelial cells requires CD14, which may complex with a Toll-like receptor (TLR) to ultimately activate NF-κB.[9] In addition, β-defensins have been recently reported to promote immune responses by recruiting dendritic and T cells through interaction with CCR6.[12]

Recently, it has been suggested that hBD-2 could be involved in the respiratory immune system.[10] Human airway epithelial cells express hBD-2, which is induced by inflammation and bacteria including *Pseudomonas aeruginosa*. It has also been demonstrated that hBD-2 has a broad spectrum of antimicrobial activity against both bacteria[6,13] and fungi,[6] which are common pathogens provoking respiratory infection. Therefore, it is postulated that hBD-2 is an epithelium-derived antimicrobial peptide that contributes to respiratory host defence.[10]

In the current study, we examined the molecular mechanisms of hBD-2 expression *in vitro*. To perform the present study, we used a human airway cell line, LC-2/ad, which was established from pleural effu-

sion of pulmonary adenocarcinoma and exhibits an epithelial appearance.[14]

MATERIALS AND METHODS

All materials were obtained from Sigma Chemical Co. (St. Louis, MO, USA) unless otherwise noted.

Cell culture

LC2/ad were obtained from RIKEN (Ibaraki, Japan) and grown in RPMI 1640 (Nissui, Tokyo, Japan)/ Ham F12 (Nissui) medium containing 15% fetal bovine serum (FBS).[14] LC2/ad from passage 3–10 were grown to confluency in $78.54 \, cm^2$ culture dishes (100 mm in diameter). The entire apparatus was placed in a CO_2 incubator at 37°C in 5% CO_2/95% humidified air.

The effect of lipopolysaccharide on human β-defensin-2 gene expression

LC2/ad were stimulated with *Pseudomonas aeruginosa*-derived LPS, serotype 10. A time course of hBD-2 mRNA induction by LPS (1 μg/mL) was performed from 0 to 48 h. Dose-dependent responses induction of hBD-2 mRNA by LPS was examined at 24 h. We aspirated medium from culture dishes after stimulation with LPS and washed the cells twice. RNA was extracted frin each sample and analysed by Northern blot.

Regulation of human β-defensin-2 by transcriptional factors and intracellular calcium chelator

To study the role of NF-κB in LPS-induced hBD-2 gene expression, pyrrolidine dithiocarbamate (PDTC), an NF-κB inhibitor, was added to the medium. The concentration of FBS in the medium was 5% during the experiments. LC2/ad were pretreated with PDTC for 2 h and subsequently stimulated with LPS for 12 h.

The role of AP-1 in the LPS-induced hBD-2 gene expression was examined by adding 12-*O*-tetradecanoylphorbol-13-acetate (TPA) to the medium. LC2/ad were stimulated with TPA (10^{-7} M) for indicated times. In addition, LC2/ad were pretreated with TPA (10^{-7} M) for 24 h and subsequently stimulated with LPS (1 μg/mL) for 1–24 h.

In order to elucidate the role of intracellular calcium in LPS-induced elevation of hBD-2 gene expression, bis-(o-aminophenoxy)-ethane-N,N, N′,N′–tetraacetic acid, tetra (acetoxymethyl)-ester (BAPTA-AM, intracellular calcium chelator) (Dojin Chemical Institute, Kumamato, Japan) was added to the medium. LC2/ad were pretreated with BAPTA-AM for 2 h and subsequently stimulated with LPS (1 μg/mL) for 24 h.

Regulation of human β-defensin-2 by glucocorticoids

In order to study the effects of glucocorticoids, a range of dexamethasone concentrations were added to the medium. LC2/ad were pretreated with dexamethasone for 2 h and subsequently stimulated with LPS (1 μg/mL) for 24 h. RNA was extracted frin each sample and analysed by Northern blot.

### Regulation of human β-defensin-2 by cyclooxygenase inhibitors

In order to study the effects of COX inhibitors, indomethacin, aspirin or NS-398 (Cayman Chemical, MI, USA) were added to the medium. LC2/ad were pretreated with each COX inhibitor for 2 h and subsequently stimulated with LPS (1 μg/mL) for 24 h.

Reverse transcription polymerase chain reaction amplification

The reverse transcription polymerase chain reaction (RT-PCR) hBD-2 cDNA product was obtained by using oligonucleotides, 5′-CCAGCCATCAGCCATGAG GGT-3′ as an antisense primer, 5′-GGAGCCCTTTCT GAATCGCA-3′ as a sense primer, and RNA from LC2/ ad cells as a template. The RT-PCR was performed using a Titan one tube RT-PCR kit. The general protocol for RT-PCR amplification was modified as follows: initial denaturation was 1 min at 95°C; 40 cycles of amplification was performed by cycling 1.15 min at 94°C, 30 s at 60°C, and 1 min at 68°C. Bands were purified by electroelution after electrophoresis in polyacrylamide gels.

Human β-defensin-2 cDNA probe and Northern blot analysis

The above-mentioned RT-PCR amplification was used to generate an hBD-2 cDNA fragment. The human β-defensin-2 cDNA fragment was ligated into pCR 2.1 vector (Invitrogen, Carlsbad, CA, USA). We aspirated medium from culture dishes stimulated with various drugs and then washed the cells twice. Total cellular RNA was extracted by the acid guanidinium thyocynate-phenol-chloroform method[15] from LC2/ad and quantitated by measuring absorbance at 260 nm. RNA samples (25 μg) were electrophoresed through 1.2% formaldehyde/agarose gels and transferred to nylon membranes (Biodyne Plus Membrane, PALL Corporation, Hills, NY, USA) by standard procedures.[16] The membranes were hybridized with a random primed, ^{32}P-labelled, Eco RI fragment of hBD-2 cDNA. The hybridization was performed for 2 h using Quick Hybridization Solution (Stratagene, La Jolla, CA, USA). The hybridized membranes were then washed and autoradiographed. The membranes were subsequently rehybridized with a ^{32}P-labelled 18S oligonucleotide

(a)

(b)
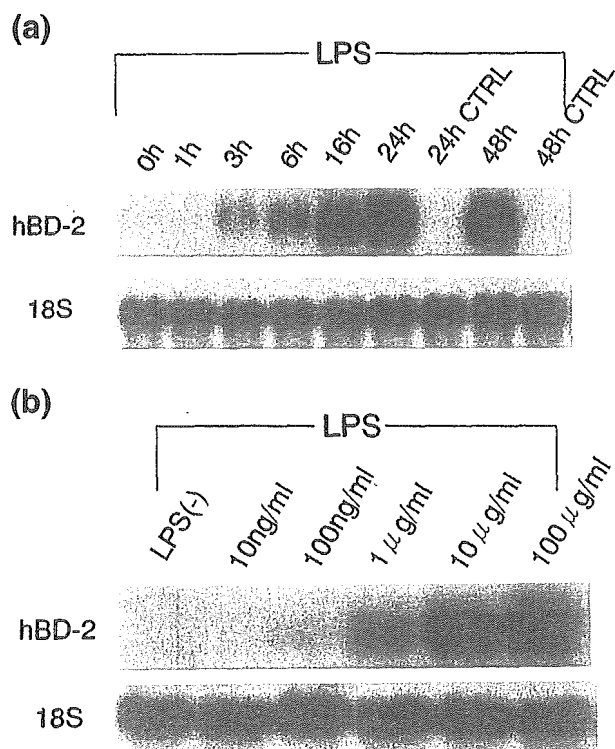
Figure 1 (a) Time course of human β-defensin-2 (hBD-2) mRNA induction by lipopolysaccharide (LPS). The human airway cell line LC2/ad was stimulated by LPS (10 μg/mL), and total RNA was extracted at the indicated times. Northern blot analysis was performed with 25 μg of total RNA hybridized with hBD-2 cDNA probe. The membrane was rehybridized with 18S probe. (b) Dose responses of hBD-2 mRNA induction by LPS. LC2/ad were stimulated with LPS, and total RNA was extracted after 24 h. Northern blot analysis was performed with 25 μg of total RNA hybridized with hBD-2 cDNA probe. The membrane was rehybridized with 18S probe.

(ACGGTATCTGATCGTCTTCGAACC) as an internal standard for total RNA content.

RESULTS

The baseline level of hBD-2 mRNA was not detectable, while LPS increased hBD-2 mRNA levels in LC2/ad in both a time- (Fig. 1a) and dose-dependent manner (Fig. 1b). Lipopolysaccharide-induced elevation of hBD-2 mRNA was inhibited by PDTC (NF-κB inhibitor).

To study the role of NF-κB in LPS-induced hBD-2 gene expression, LC2/ad were pretreated with PDTC for 2 h and subsequently stimulated with LPS for 12 h. Lipopolysaccharide-induced elevation of hBD-2 mRNA was partially inhibited by PDTC pretreatment, suggesting that LPS-induced elevation of hBD-2 gene expression is dependent on NF-κB activity in part (Fig. 2).

LC2/ad were then stimulated by TPA (10^{-7} M). While increased mRNA levels of heparin-binding epidermal
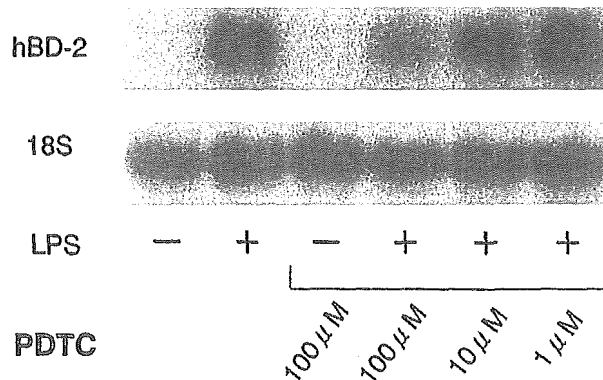
Figure 2 Lipopolysaccharide (LPS)-induced up-regulation of human β-defensin-2 (hBD-2) mRNA was inhibited by a NF-κB inhibitor, pyrrolidine dithiocarbamate (PDTC). LC2/ad cells were stimulated with LPS (1 μg/mL) in the absence or presence of PDTC for 12 h. Northern blot analysis was performed with 25 μg of total RNA hybridized with hBD-2 cDNA probe. The membrane was rehybridized with 18S probe.

growth factor like growth factor (HB-EGF) were observed following 1–4 h TPA pretreatment, hBD-2 gene expression was not detected at any time point (Fig. 3a). This result indicated that TPA stimulation was sufficient for the induction of HB-EGF, but not for that of hBD-2. LC2/ad were pretreated with TPA (10^{-7} M) for 24 h to down-regulate protein kinase C (PKC) activity. Cells were subsequently stimulated with LPS for 1–24 h. Lipopolysaccharide-induced elevation of hBD-2 mRNA was inhibited by TPA pretreatment, suggesting that LPS-induced elevation of hBD-2 gene expression is partly dependent on PKC activity (Fig. 3b).

To examine the role of intracellular calcium in LPS-induced up-regulation of hBD-2 gene, LC2/ad were stimulated with LPS in the absence or presence of BAPTA-AM, an intracellular calcium chelator. Lipopolysaccharide-induced elevation of hBD-2 mRNA levels was completely inhibited by BAPTA-AM (Fig. 4). This finding suggests that intracellular calcium is necessary for LPS-induced hBD-2 gene expression.

Subsequently, LC2/ad were stimulated with LPS in the absence or presence of dexamethasone (glucocorticoid), indomethacin, aspirin (COX inhibitor), and NS-398 (COX-2 selective inhibitors). As shown in Fig. 5, LPS-induced elevation of hBD-2 mRNA levels was inhibited by dexamethasone. In contrast, LPS-induced hBD-2 gene expression was not affected by indomethacin, aspirin, or NS-398 (Figs 6,7).
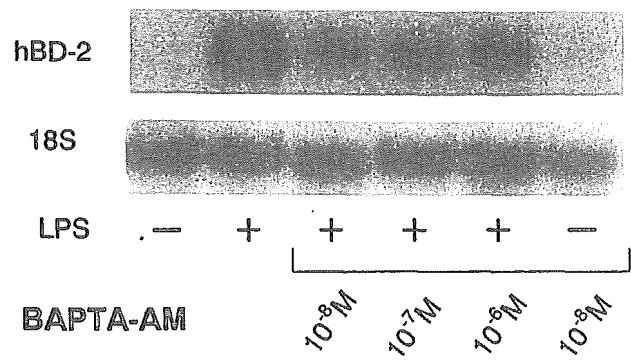
DISCUSSION

The current data indicate that dexamethasone down-regulates LPS-induced hBD-2 gene expression in airway epithelial cells. The NF-κB pathway appears to play a key role in the expression of hBD-2, while intracellular calcium and, in part, PKC activity are also essential for LPS-induced expression of hBD-2.

(a)

(b)

Control   TPA pretreatment
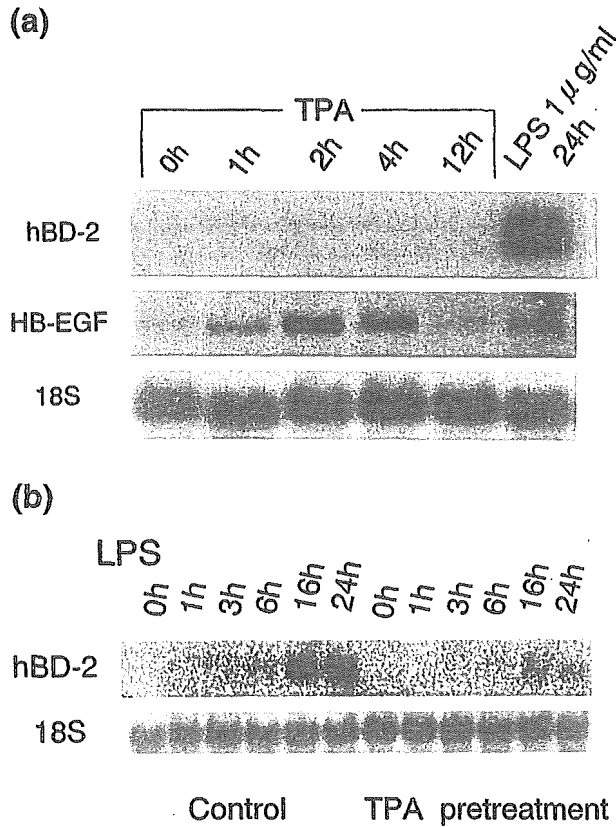
Figure 3 (a) TPA induced the expression of HB-EGF mRNA, but not that of human β-defensin-2 (hBD-2). LC2/ad were stimulated by 12-O-tetra-decanoylphorbol-13-acetate (TPA; 10^{-7} M) for the indicated times, or with lipopolysaccharide (LPS) for 24 h. Northern blot analysis was performed with 25 μg of total RNA hybridized with hBD-2 cDNA probe. The membrane was rehybridized with HB-EGF probe and 18S probe. (b) LPS-induced up-regulation of hBD-2 mRNA was partially inhibited by TPA pretreatment. LC2/ad were pretreated with TPA (10^{-7} M) for 24 h and subsequently stimulated with LPS (1 μg/mL) for 1–24 h. Northern blot analysis was performed with 25 μg of total RNA hybridized with hBD-2 cDNA probe. The membrane was rehybridized with 18S probe.

Figure 4 Lipopolysaccharide (LPS)-induced up-regulation of human β-defensin-2 (hBD-2) mRNA was inhibited by bis-(o-aminophenoxy)-ethane-N,N,N′,N′-tetraacetic acid, tetra (acetoxymethyl)-ester (BAPTA-AM). LC2/ad were stimulated with LPS (1 μg/mL) in the absence or presence of BAPTA-AM for 24 h. Northern blot analysis was performed with 25 μg of total RNA hybridized with hBD-2 cDNA probe. The membrane was rehybridized with 18S probe.
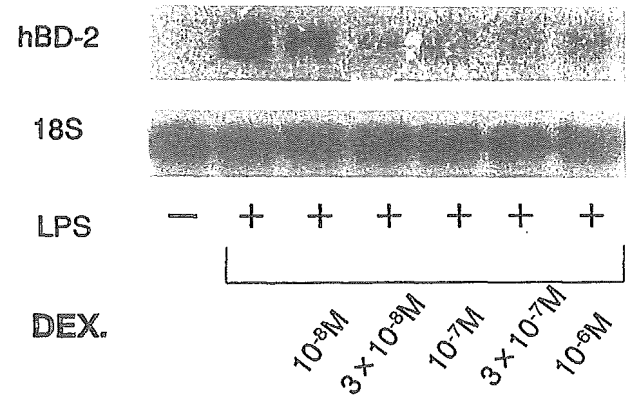
Figure 5 Lipopolysaccharide (LPS)-induced up-regulation of human β-defensin-2 (hBD-2) mRNA was inhibited by dexamethasone. LC2/ad were stimulated with LPS (1 μg/mL) in the absence or presence of dexamethasone for 24 h. Northern blot analysis was performed with 25 μg of total RNA hybridized with hBD-2 cDNA probe. The membrane was rehybridized with 18S probe. DEX, dexamethasone.

In contrast, COX inhibitors had no effect on LPS-induced hBD-2 gene expression.

β-defensins are antimicrobial peptides that control the defence of mammalian epithelial mucosa. Tracheal antimicrobial peptide (TAP) and lingual antimicrobial peptide (LAP) were the first members of the β-defensin family of mammalian antimicrobial peptides to be described.[17,18] Tracheal antimicrobial peptide is produced by bovine respiratory tract mucosa, while LAP is produced by tongue mucosa. The genes for these peptides are inducibly expressed by various proinflammatory agents such as TNF-α, IL-1β, bacteria or bacterial LPS.[19–21] In humans, three β-defensins have been identified. The first human β-defensin, hBD-1, was isolated as a trace peptide from human haemofiltrates, where its mRNA is found to be predominantly expressed in epithelia of the urogeni-

tal tract.[3–5] The second human β-defensin, hBD-2, is isolated from psoriatic skin, where its mRNA is found to be predominantly expressed in epithelia of the trachea and lung.[6,8] The third β-defensin, hBD-3, was also isolated from psoriatic skin.[7] In terms of patterns of gene expression, there is a marked difference among these β-defensins. The expression of hBD-1 has been reported to be constitutive.[4] In contrast, hBD-2 gene expression is inducible by various proinflammatory agents such as TNF-α, IL-1β, IL-8, LPS, bacteria, and yeasts.[6,8–11] The expression pattern of hBD-3 has also been reported to be inducible.[7] Therefore, hBD-2 and hBD-3 are considered to represent the human equivalent of bovine TAP and LAP. It has been suggested that these inducible β-defensins
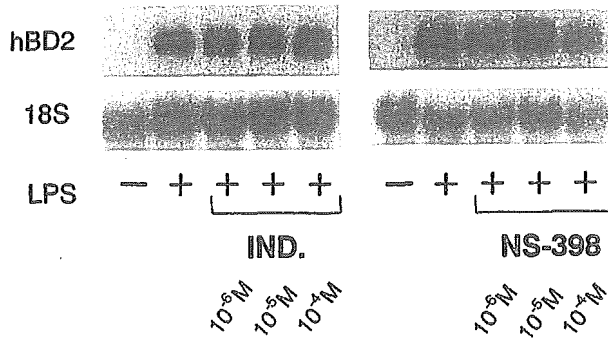
Figure 6 Lipopolysaccharide (LPS)-induced up-regulation of human β-defensin-2 (hBD-2) mRNA was not inhibited by indomethacin or NS-398. LC2/ad were stimulated with LPS (1 μg/mL) in the absence or presence of indomethacin or NS-398 for 24 h. Northern blot analysis was performed with 25 μg of total RNA hybridized with hBD-2 cDNA probe. The membrane was rehybridized with 18S probe. IND, indomethacin.
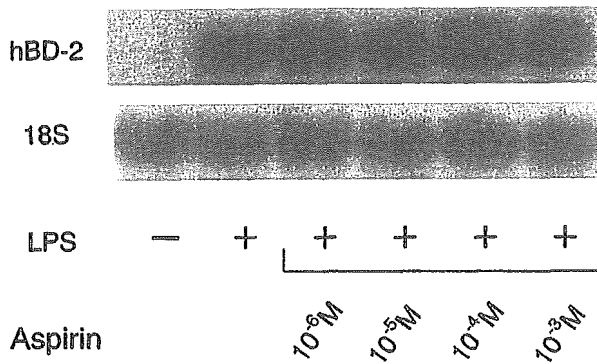
Figure 7 Lipopolysaccharide (LPS)-induced up-regulation of human β-defensin-2 (hBD-2) mRNA was not inhibited by aspirin. LC2/ad were stimulated with LPS (1 μg/mL) in the absence or presence of aspirin for 24 h. Northern blot analysis was performed with 25 μg of total RNA hybridized with hBD-2 cDNA probe. The membrane was rehybridized with 18S probe.

may play important roles in innate immunity and dynamic host defence.

Recently, the 5′-flanking region of hBD-2 has been demonstrated to contain consensus binding sequences for AP-1-like and NF-κB-like sites, suggesting that hBD-2 is inducible by acute inflammatory stimuli. Consequently, it has been assumed that AP-1 and NF-κB participate in transcriptional regulation. In support of this, it was reported that NF-κB participates in the transcriptional regulation of TAP gene expression following LPS stimulation.[21] Furthermore, it has been recently reported that LPS-induced expression of hBD-2 in human tracheobronchial epithelial cells requires CD14 and Toll-like receptors (TLR) to activate NF-κB.[9] It is presumed that: (i) mammalian TLR and associated signalling factors may represent a conserved evolutionary response to infec-

tious pathogens, and (ii) LPS- and IL-1-inducible hBD-2 may be a conserved defence mechanism similar to the antimicrobial peptides found in Drosophila.[22] However, little is yet known about roles of AP-1 in hBD-2 expression. From the present study it is suggested that transcriptional activity of hBD-2 is related to NF-κB and, partly, AP-1. This finding is compatible with the existence of both consensus sequences in the putative promoter region. In addition, intracellular calcium is also involved in hBD-2 gene expression induced by LPS.

Glucocorticoids have been used as immunosuppressive drugs to manage inflammatory diseases. It is postulated that the activities of GC are mediated by (i) various transcription factors including NF-κB and AP-1 and (ii) T-cell-mediated immunity. While GC are useful immunosuppressive agents, high doses of GC are associated with a high incidence of infection. Currently, little is known about GC-induced susceptibility to opportunistic infection. In the present study, we obtained direct evidence that LPS-induced hBD-2 gene expression was inhibited by dexamethasone in airway epithelial cells *in vitro*.

It is possible that GC-induced down-regulation of hBD-2 is related to the increased risk of opportunistic respiratory infection in GC-treated patients. Glucocorticoids inhibit both NF-κB and AP-1 transcription factors, resulting in inhibition of hBD-2 gene expression. Since hBD-2 has both bactericidal and fungicidal activities,[6,14] GC-induced inhibition of hBD-2 might contribute to opportunistic respiratory infection. In addition, previous reports have shown that β-defensins including hBD-2 are chemotactic for immature dendritic cells and memory T cells through CCR6.[12] Therefore, GC-induced inhibition of hBD-2 is potentially involved in suppression of T-cell-mediated host defence.

In the present study, COX inhibitors including a COX-2 selective inhibitor had no effect on LPS-induced hBD-2 gene expression in cultured airway epithelial cells. It remains controversial whether host defence against infectious agents would be affected by non-steroidal anti-inflammatory drugs including COX inhibitors. The present results suggest that COX inhibitors are unlikely to suppress defence mechanisms associated with hBD-2 in airway epithelia. Recently it has been reported that inhibition of COX and lipoxygenase might be effective in treating sepsis-associated adult respiratory distress syndrome.[23] The present data might further support this treatment in terms of maintaining host defence.

In summary, dexamethasone inhibits hBD-2 gene expression induced by LPS. Both NF-κB and AP-1 transcription factors are essential for hBD-2 gene expression. Cyclooxygenase inhibitors fail to inhibit LPS-induced expression of hBD-2, suggesting that COX inhibitors are unlikely to suppress host defence associated with hBD-2. Glucocorticoid-induced down-regulation of hBD-2 may be related to GC-induced suppression of respiratory host defence. The inducible β-defensins including hBD-2 might provide a new therapeutic approach to GC-induced susceptibility to respiratory infection.

REFERENCES

1 Hancock REW. Peptide antibiotics. *Lancet* 1997; **349**: 418–22.

2 Ganz T. Defensins and host defence. *Science* 1999; **286**: 420–1.

3 Bensch KW, Raida M, Magert HJ, Schulz-Knappe P, Forssmann W. hBD-1: a novel β-defensin from human plasma. *FEBS Lett.* 1995; **368**: 331–5.

4 Zhao C, Wang I, Lehrer RI. Widespread expression of beta-defensin hBD-1 in human secretory glands and epithelial cells. *FEBS Lett.* 1996; **396**: 319–22.

5 Valore EV, Park CH, Quayle AJ, Wiles KR, McCray PB, Ganz T. Human β-defensin-1: an antimicrobial peptide of urogenital tissues. *J. Clin. Invest.* 1998; **101**: 1633–42.

6 Harder J, Bartels J, Christophers E, Schröder JM. A peptide antibiotic from human skin. *Nature* 1997; **387**: 861.

7 Harder J, Bartels J, Christophers E, Schröder JM. Isolation and characterization of human β-defensin-3, a novel human inducible peptide antibiotic. *J. Biol. Chem.* 2000; **276**: 5707–13.

8 Singh PK, Jia HP, Wiles K *et al.* Production of β-defensins by human airway epithelia. *Proc.Natl Acad. Sci. USA* 1998; **95**: 14961–6.

9 Becker MN, Diamond G, Verghese MW, Randell SH. CD14-dependent LPS-induced β-defensin-2 expressed in human tracheobronchial epithelium. *J. Biol. Chem* 2000; **275**: 29731–6.

10 Harder J, Meyer-Hoffert U, Teran LM *et al.* Mucoid *Pseudomonas aeruginosa*, TNFα, and IL-1β, but not IL-6, induce human β-defensin-2 in respiratory epithelia. *Am. J. Respir. Cell Mol. Biol.* 2000; **22**: 714–21.

11 Krisanaprakornkit S, Kimball JR, Weinberg A, Darveau RP, Bainbridge BW, Dale BA. Inducible expression of human β-defensin 2 by *Fusobacterium nucleatum* in oral epithelial cells. multiple signaling pathways and role of commensal bacteria in innate immunity and the epithelial barrier. *Infect. Immun.* 2000; **68**: 2907–15.

12 Yang D, Chertov O, Bykovskaia SN *et al.* β-defensins: linking innate and adaptive immunity through dendritic and T cell CCR6. *Science* 1999; **286**: 525–8.

13 Tomita T, Hitomi S, Nagase T, Matsui H, Matsuse T, Kimura S, Ouchi Y. Effect of ions on antibacterial activity of human beta defensin 2. *Microbiol. Immunol.* 2000; **44**: 749–54.

14 Kataoka H, Itoh H, Seguchi K, Koono M. Establishment and characterization of a human lung adenocarcinoma cell line (LC-2/ad) producing α_1-antitrypsin in vitro. *Acta Pathol. Jpn.* 1993; **43**: 566–73.

15 Chomczynski P, Sacchi N. Single-step method of RNA isolation by acid guanidinium thiocyanate-phenol chloroform extraction. *Anal. Biochem.* 1987; **162**: 156–9.

16 Sambrook J, Fritsch EF, Maniatis T. *Molecular Cloning: a Laboratory Manual*, 2nd edn. Cold Spring Harbor Laboratory, Cold Spring Harbor, NY, 1989.

17 Diamond G, Zasloff M, Eck H, Brasseur M, Maloy WL, Bevins CL. Tracheal antimicrobial peptide, a cystine-rich peptide from mammalian tracheal mucosa: peptide isolation and cloning of a cDNA. *Proc. Natl Acad. Sci. USA* 1991; **88**: 3952–6.

18 Schonwetter BS, Stolzenberg ED, Zasloff MA. Epithelial antibiotics induced at sites of inflammation. *Science* 1995; **267**: 1645–8.

19 Diamond G, Russell JP, Bevins CL. Inducible expression of an antibiotic peptide gene in lipopolysaccharide-challenged tracheal epithelial cells. *Proc. Natl Acad. Sci. USA* 1996; **93**: 5156–60.

20 Russel JP, Diamond G, Tarver AP, Scanlin TF, Bevins CL. Coordinate induction of two antibiotic genes in tracheal epithelial cells exposed to the inflammatory mediators lipopolysaccharide and tumor necrosis factor alpha. *Infect. Immun.* 1996; **64**: 1565–8.

21 Diamond G, Kaiser V, Rhodes J, Russell JP, Bevins CL. Transcriptional regulation of β-defensin gene expression in tracheal epithelial cells. *Infect. Immun.* 2000; **68**: 113–19.

22 Tan BH, Modlin RL. Drosophila, the savvy exterminator. *Nat. Immunol.* 2000; **1**: 361.

23 Nagase T, Uozumi N, Ishii S *et al.* Acute lung injury by sepsis and acid aspiration: a key role for cytosolic phospholipase A2. *Nat. Immunol.* 2000; **1**: 42–6.

A pivotal role of cytosolic phospholipase A_2 in bleomycin-induced pulmonary fibrosis

TAKAHIDE NAGASE[1], NAONORI UOZUMI[2,3], SATOSHI ISHII[2,3], YOSHIHIRO KITA[2,3], HIROSHI YAMAMOTO[1], EIJIRO OHGA[1], YASUYOSHI OUCHI[1] & TAKAO SHIMIZU[2,3].

[1]Department of Geriatric Medicine; [2]Department of Biochemistry and Molecular Biology, Graduate School of Medicine, University of Tokyo, Tokyo, Japan
[3]CREST of Japan Science and Technology Corporation, Tokyo, Japan
Correspondence should be addressed to T.N.; email: takahide-tky@umin.ac.jp

Pulmonary fibrosis is an interstitial disorder of the lung parenchyma whose mechanism is poorly understood. Potential mechanisms include the infiltration of inflammatory cells to the lungs and the generation of pro-inflammatory mediators. In particular, idiopathic pulmonary fibrosis is a progressive and fatal form of the disorder characterized by alveolar inflammation, fibroblast proliferation and collagen deposition. Here, we investigated the role of cytosolic phospholipase A_2 (cPLA$_2$) in pulmonary fibrosis using cPLA$_2$-null mutant mice, as cPLA$_2$ is a key enzyme in the generation of pro-inflammatory eicosanoids. Disruption of the gene encoding cPLA$_2$ (Pla2g4a) attenuated IPF and inflammation induced by bleomycin administration. Bleomycin-induced overproduction of thromboxanes and leukotrienes in lung was significantly reduced in cPLA$_2$-null mice. Our data suggest that cPLA$_2$ has an important role in the pathogenesis of pulmonary fibrosis. The inhibition of cPLA$_2$-initiated pathways might provide a novel therapeutic approach to pulmonary fibrosis, for which no pharmaceutical agents are currently available.

Pulmonary fibrosis comprises a group of interstitial disorders of the lung parenchyma[1-5]. Idiopathic pulmonary fibrosis (IPF) is the most common form of the disorder and is characterized by progressive development of alveolar inflammation, fibroblast proliferation and collagen deposition. IPF is clinically manifested as increased lung elasticity, restrictive ventilation impairment and respiratory failure[1]. Although IPF is a progressive and fatal disease, no useful drugs are currently available for its treatment. Current medical intervention for IPF is either lung transplantation or supportive treatment, such as oxygen therapy. Although the molecular mechanisms underlying development of IPF remains to be elucidated, potential mechanisms might be the infiltration of inflammatory cells to the lungs, and the generation of pro-inflammatory and proliferative mediators, leading to fibroblast proliferation and accumulation of extracellular collagen[1,2].

Platelet-activating factor (PAF) and metabolites of arachidonic acid might be involved in pathogenesis of pulmonary fibrosis, although little attention has been paid to these mediators. PAF is a pro-inflammatory phospholipid mediator that has various biological effects including cell proliferation and the production of cytokines and eicosanoids via activation of the G protein–coupled PAF receptor (PAFR)[6-17]. Thromboxanes (Txs) and leukotrienes (LTs) are potent mediators generated from arachidonic acid by cyclooxygenase and 5-lipoxygenase, respectively. TxA$_2$ may induce lung inflammation, whereas LTB$_4$ is a potent neutrophil chemoattractant. Cysteinyl LTs (LTC$_4$, LTD$_4$ and LTE$_4$) are among the most important mediators in inflammatory lung diseases. A crucial enzyme for generation of these pro-inflammatory mediators, including eicosanoids and PAF, is phospholipase A$_2$. In particular, cytosolic phospholipase A$_2$ (cPLA$_2$) is a key player, as it is activated by submicromolar concentration of Ca^{++} and by phosphorylation by mitogen-activated protein kinases[18-22].

Our aim was to elucidate the role of cPLA$_2$ in the experimental model of pulmonary fibrosis induced by bleomycin. To perform this study, we used mutant mice lacking the gene encoding cPLA$_2$ (ref. 23; also known as Pla2g4a) and their wild-type littermates as controls.

Pulmonary fibrosis induced by bleomycin administration

Fig. 1 demonstrates the lung elasticity in bleomycin and saline-treated groups (n = 4–6). In the bleomycin-treated wild-type group, the value of lung elastance (EL) was significantly greater than those in the other groups, whereas there was a no difference in EL values among bleomycin-treated cPLA$_2$-null group and saline-treated groups. In terms of alterations in lung parenchyma, physiological data suggest that bleomycin-induced responses in cPLA$_2$-null mice were significantly reduced compared with their wild-type controls.

We assessed collagen content of the lungs by measuring hydroxyproline-content values. Values in bleomycin-treated wild-type group were significantly greater than those in bleomycin-treated cPLA$_2$-null group (83.6 ± 4.4 and 56.0 ± 3.0 μg per left lung; n = 6, respectively; $P < 0.05$), indicating that bleomycin-induced collagen synthesis in cPLA$_2$-null mice was significantly attenuated compared with bleomycin-treated wild-type group. There was no difference in hydroxyproline content among bleomycin-treated cPLA$_2$-null group and saline-treated groups.

Histopathological assessment of pulmonary fibrosis

Fig. 2 shows lung histology 14 days after bleomycin or saline
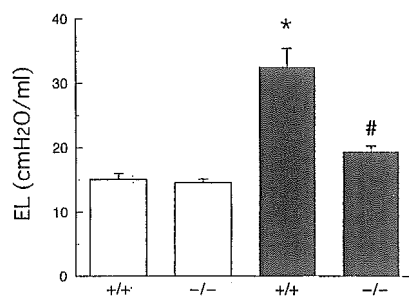
Fig. 1 Physiological roles of cPLA$_2$ in IPF induced by bleomycin treatment. Responses in EL 14 d after the administration of bleomycin (■) or saline (□) in the wild-type (+/+) or cPLA$_2$-null (–/–)mice (n = 4–6). *, $P < 0.001$ versus saline-treated; #, $P < 0.001$ versus bleomycin-treated wild-type group.

administration. Bleomycin treatment elicited alveolar thickening and subpleural fibrous foci in wild-type mice. In cPLA$_2$-null mice, histological changes including alveolar thickening and fibrosis were minimal. We performed further histopathological evaluation of pulmonary fibrosis using an established scoring method[3]. There was a significant difference in the scores of fibrotic lesions between bleomycin-treated wild-type and cPLA$_2$-null mice (Fig. 3).

Bleomycin-induced inflammation

In the wild-type group, bleomycin administration increased protein content and the numbers of macrophages, polymorphonuclear leukocytes (PMNs) and lymphocytes in bronchoalveolar lavage fluid (BALF), indicating bleomycin-induced protein leakage and leukocyte infiltration (Table 1 and Fig. 4). The protein leakage was significantly attenuated in cPLA$_2$-null mice, which had lesser macrophage, PMN and lymphocyte sequestration compared with the control mice (Fig. 4).

Thromboxane and leukotriene content

To assess the biosynthesis of cPLA$_2$ products, we performed BALF assays of TxA$_2$ (measured as TxB$_2$), LTB$_4$ and LTC$_4$/D$_4$/E$_4$. Table 1 summarizes the results of BALF TxB$_2$, LTB$_4$ and LTC$_4$/D$_4$/E$_4$ assays in each experimental group. Each eicosanoid level in bleomycin-treated wild-type mice was significantly

greater than that in any other group, whereas any eicosanoid measured in similarly treated cPLA$_2$-null mice was reduced to the same level as the saline-treated groups. Bleomycin administration increased TxB$_2$, LTB$_4$ and LTC$_4$/D$_4$/E$_4$ levels in BALF, whereas the levels of these eicosanoids were significantly reduced in cPLA$_2$-null mice.

Relative contribution of downstream cPLA$_2$ mediator, PAF

To assess the relative contribution of downstream mediators of cPLA$_2$, we examined the role of PAF in bleomycin-induced pulmonary fibrosis using mutant mice lacking the gene encoding the PAF receptor (Pafr^{–/–} mice)[17] and their wild-type littermates as controls. The disruption of Pafr reduced the score of fibrotic lesions, although there was a marked difference between bleomycin-treated Pafr^{–/–} mice and saline-treated groups (Table 2). However, there was no significant difference in either EL or hydroxyproline content between bleomycin-treated wild-type and Pafr^{–/–} mice.

Discussion

Our results suggest that cPLA$_2$ has a pivotal role in the pathogenesis of pulmonary fibrosis. Disruption of the gene encoding cPLA$_2$ significantly attenuated pulmonary fibrosis and inflammation induced by bleomycin. These observations indicate that cPLA$_2$ may be involved in pulmonary fibrosis by mediating overproduction of inflammatory mediators including Txs and LTs.

The fibrotic lung disorders such as IPF are characterized by chronic lung parenchymal injury and inflammation, that is, alveolitis[1,2]. The inflammation of pulmonary fibrosis is associated with infiltration of leukocytes including macrophages, lymphocytes and neutrophils. It is thought that these inflammatory cells might generate and release chemical mediators, leading to proliferation of mesenchymal cells and deposition of extracellular matrix protein. This pathologic process is associated with clinical findings including reduced vital capacity and impaired gas exchange[1]. In investigating the pathogenesis of pulmonary fibrosis, the efficacy of the pharmacological approach is limited as the progression of fibrotic disorders is a chronic and continuous process. We therefore used a mutant mouse model to examine whether cPLA$_2$ would mediate development of IPF.

In bleomycin-treated wild-type mice, we observed increases in EL, pulmonary fibrosis, protein leakage and infiltration of inflammatory cells including macrophages, lymphocytes and

Table 1 Physiological and biochemical data after saline or bleomycin treatment

Mouse type/ Treatment	EL (cmH$_2$O/ml)	BALF total protein (mg)	BALF total cell counts (× 10^4)	BALF total TxB$_2$ (ng)	BALF total LTB$_4$ (ng)	BALF total LTC$_4$/D$_4$/E$_4$ (ng)
Wild type Saline	14.5 ± 0.2	0.122 ± 0.006	9.9 ± 0.8	0.011 ± 0.011	0.000 ± 0.000	1.103 ± 0.144
cPLA$_2$-null Saline	15.4 ± 0.8	0.129 ± 0.011	8.5 ± 0.8	0.000 ± 0.000	0.000 ± 0.000	0.281 ± 0.169
Wild type Bleomycin	33.0 ± 3.0*	0.703 ± 0.142[†]	63.1 ± 6.1*	0.077 ± 0.018*	0.026 ± 0.005*	23.400 ± 5.201*
cPLA$_2$-null Bleomycin	20.0 ± 1.1[#]	0.224 ± 0.073[#]	23.4 ± 1.3[#]	0.015 ± 0.009[#]	0.000 ± 0.000[#]	1.838 ± 0.643[#]

Data collected 7 d after treatment. [†], $P < 0.05$; *, $P < 0.01$ versus saline-treated groups; [#], $P < 0.01$ versus bleomycin-treated wild-type group (n = 4–7).
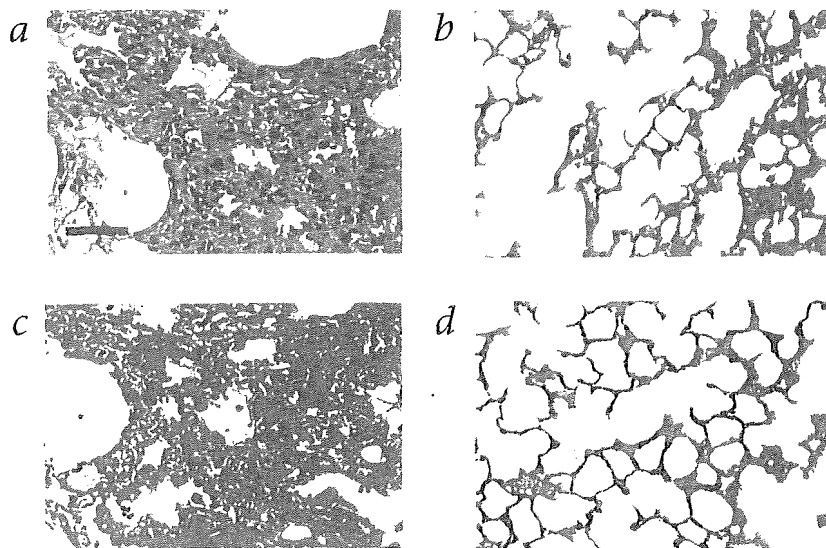
Fig. 2 Photomicrograph of lung tissues from wild-type and cPLA$_2$-null mice 14 d after bleomycin administration. *a–d*, In wild-type mice, there was marked accumulation of neutrophils and collagen (*a* and *c*), while there were little histological changes in cPLA$_2$-null (*b* and *d*). *a* and *b*, H&E stain; *c* and *d*, Masson's trichrome stain. Scale bar, 50 μm.

brosis, but the LTC$_4$/D$_4$/E$_4$ levels were much higher than the other eicosanoids. As there is abundant cysteinyl LT receptors in the lung[27], the coupling of these cysteinyl LTs and receptors may induce inflammatory process including increased permeability and leukocyte infiltration in the lung[28]. Our findings suggest that the cysteinyl LTs might have an important role in the development of pulmonary fibrosis.

Recent studies have shown that cPLA$_2$ may be involved in the pathogenesis of various inflammatory diseases including bronchial asthma and adult respiratory distress syndrome (ARDS)[23,29]. Although there are extreme differences in clinical features between ARDS and IPF, both diseases are fatal disorders with no useful drug therapies. Whereas no effective cPLA$_2$ inhibitors are available, cPLA$_2$ might be a potential target to intervene development of pulmonary fibrosis as well as acute lung injury.

Bleomycin is an antibiotic agent with antitumor activity and commonly used to treat various types of tumors[30]. It has been reported that bleomycin is an essential component of combination chemotherapy in patients with germ-cell tumors[31]. The most important and severe side effects of bleomycin are pulmonary injuries including bleomycin-induced pulmonary fibrosis[30]. In terms of both clinical and pathological features, bleomycin-induced pulmonary fibrosis resembles IPF. Histologically, bleomycin-induced pulmonary fibrosis is associated with infiltration of inflammatory cells into alveoli, focal collagen depositions and fibrotic lesions[30]. Recent studies have shown that bleomycin stimulates cytokine secretion by alveolar macrophage or fibroblast proliferation in human cells[32,33]. However, the exact mechanism underlying the development of bleomycin-induced pulmonary fibrosis also remains to be elucidated.

Notably, although disruption of the gene encoding cPLA$_2$ attenuated bleomycin-induced lung injury, it did not com-

neutrophils. Consistently, increases in Txs and LTs were found in the BAL fluid of bleomycin-treated wild-type mice. These observations were markedly attenuated by cPLA$_2$ gene disruption, suggesting that cPLA$_2$ could mediate the process of lung fibrotic disorder via the production of pro-inflammatory mediators. Moreover, cPLA$_2$ products are related to infiltration of various leukocytes, which may lead to the fibrotic disorder. Indeed, increases in leukocytes, especially PMNs, are found in BAL fluid of patients with IPF (ref. 1). It has been reported that lung homogenates from IPF patients contain much higher levels of LTB$_4$ and LTC$_4$ compared with non-fibrotic controls[2]. LTB$_4$ is an important mediator of neutrophil-mediated inflammation including lung injury[24–26]. It is possible that not only PMN, but also macrophages and lymphocytes, may be necessary to induce the bleomycin-induced lung inflammation. The cPLA$_2$-initiated pathways may mediate both infiltration and activation of these leukocytes triggered by bleomycin, resulting in pulmonary fibrosis. Our results suggest that cPLA$_2$ has a dominant role in leukocyte sequestration, and potential interaction between mediators such as PAF and eicosanoids may further upregulate the development of fibrotic process.

To investigate the relative contribution of downstream pathways of cPLA$_2$ mediators, we investigated the role of PAF in bleomycin-induced fibrosis using mutant mice established in our laboratory[17]. We observed that the disruption of the PAF receptor modestly attenuated the histopathological changes induced by bleomycin, although we found no significant differences in physiological data or collagen content between bleomycin-treated mutant mice and controls. These findings suggest that PAF may be potentially involved in the development of bleomycin-induced pulmonary fibrosis. However, the relative contribution of PAF is only partial and limited when compared with the crucial role of cPLA$_2$. We therefore suggest that other downstream mediators of cPLA$_2$, that is, eicosanoids produced by cyclooxygenase and/or lipoxygenase, may also contribute to the development of bleomycin-induced pulmonary fibrosis.
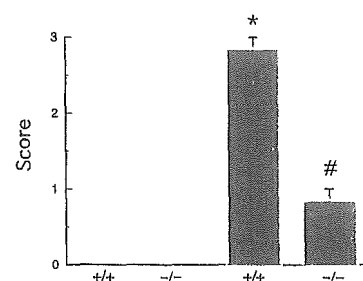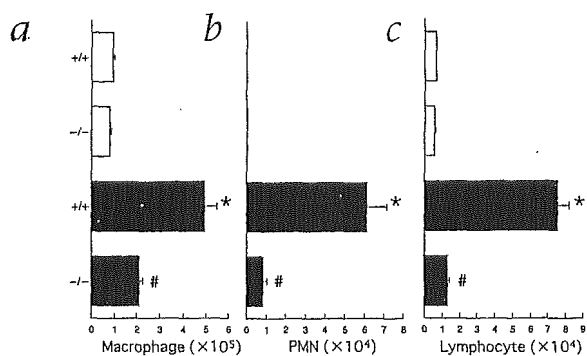
Here we measured TxB$_2$, LTB$_4$ and cysteinyl LTs (LTC$_4$, LTD$_4$ and LTE$_4$) in BALF to confirm the generation of cPLA$_2$ products. We observed significant increases in each eicosanoid in the model of bleomycin-induced pulmonary fi-

Fig. 3 Histopathological roles of cPLA$_2$ in pulmonary fibrosis induced by bleomycin treatment. Using a scoring method[3], quantitative assessment was performed 7 d after the administration of bleomycin (■) or saline (□) in the wild-type (+/+) or cPLA$_2$-null (–/–) mice ($n = 4$–6). *, $P < 0.001$ versus saline-treated; #, $P < 0.001$ versus bleomycin-treated wild-type group.

– 94 –

pletely abolish the pathology. Indeed, we found a significant difference in histopathologic scores of fibrosis between bleomycin-treated cPLA$_2$-null mice and saline-treated controls. This observation indicates that factors other than cPLA$_2$ should also be involved in the process of pulmonary fibrosis. It has been postulated that oxygen radicals, adhesion molecules, plasminogen-activator inhibitor and cytokines are also involved in this mechanism[1–5]. Because no pharmacological agents are available to treat pulmonary fibrosis and increase survival rates, these factors are also potential targets to develop agents. Our data suggest that the intervention of cPLA$_2$ may also be a promising tool to improve management of pulmonary fibrosis.

In summary, the disruption of cPLA$_2$ significantly attenuated lung inflammation and fibrosis induced by bleomycin treatment. cPLA$_2$ pathways might be involved in the pathogenesis of pulmonary fibrosis caused by bleomycin, and inhibition of these pathways may provide a novel and potential therapeutic approach to pulmonary fibrosis.

Methods

Mice. cPLA$_2$-null mice were established by gene targeting[23]. Mice heterozygous for cPLA$_2$ mutant allele with the genetic background of the C57BL/6J × 129/Ola hybrid were mated. Pafr$^{-/-}$ mice were also established as reported[17,34,35]. Offspring were genotyped at 4 wk of age. For genotyping, genomic DNAs were isolated from biopsied tail and subjected to PCR amplification[23]. The animals were maintained on a light/dark cycle with light from 7:00 to 20:00 at 25 °C. Mice were fed with a standard laboratory diet and water *ad libitum*. Mutant homozygous mice and their littermate homozygous controls were used in this study. All animal experiments were approved by the University of Tokyo Ethics Committee for Animal Experiments.

Table 2 Roles of PAF in bleomycin-induced pulmonary fibrosis

Mouse type/ Treatment	EL (cm H$_2$O/ml)	Hydroxyproline value (μg/left lung)	Score of fibrotic lesions
Wild type Saline	14.8 ± 1.1	43.2 ± 3.3	0.0 ± 0.0
Pafr$^{-/-}$ Saline	14.1 ± 1.1	43.0 ± 3.7	0.0 ± 0.0
Wild type Bleomycin	32.5 ± 2.2*	82.0 ± 7.2†	2.8 ± 0.2*
Pafr$^{-/-}$ Bleomycin	26.9 ± 2.3†	59.8 ± 12.1	2.0 ± 0.0*#

†, $P < 0.05$; *, $P < 0.001$ versus saline-treated groups; #, $P < 0.05$ versus bleomycin-treated wild-type group (*n* = 4–5).

Experimental pulmonary fibrosis induced by bleomycin administration. Mice were anesthetized with ketamine and tracheostomized. Then, 1.5 ml/kg solution containing bleomycin (5 mg/kg, Nippon Kayaku, Tokyo, Japan) was intratracheally administered. Control animals were treated with saline instead of bleomycin in the same manner. These procedures were performed in a sterile environment. To assess the development of pulmonary fibrosis physiologically, EL (a reciprocal of lung compliance) was measured 7 or 14 d after bleomycin or saline administration as described[36–40]. Briefly, we measured the tracheal pressure (*Ptr*), flow and volume (*V*). EL and lung resistance (RL, data not shown) were calculated by adjusting the equation of motion: $Ptr = EL (V) + RL (dV/dt) + K$, where K was a constant. Values in EL reflect lung parenchymal alterations and stiffening of the lungs.

Assessment of collagen synthesis. To assess collagen synthesis, a hydroxyproline assay was performed. Mice were anesthetized and the lungs were removed 14 d after bleomycin or saline treatment. The left lung was then excised and hydroxyproline content was measured as reported[3].

Histopathological assessment of pulmonary fibrosis. The right lung of each animal was excised 14 d after bleomycin or saline treatment. Following fixation, the tissue blocks obtained from midsagittal slices of the lungs were embedded in paraffin. The slices were stained with H&E or with Masson's trichrome stain. Histopathological evaluation of pulmonary fibrosis was performed using a scoring method as described[3]. Briefly, the scores of fibrotic lesions were defined as follows: 0, absence of lesion; 1, occasional small localized subpleural foci; 2, thickening of interalveolar septa and subpleural foci; 3, thickened continuous subpleural fibrosis and interalveolar septa.

Bronchoalveolar lavage fluid. 7 d after bleomycin or saline treatment, bronchoalveolar lavage (BAL) was performed (1 ml PBS × 5). In each animal, 90% (4.5 ml) of the total injected volume was consistently recovered. After BAL fluid was centrifuged at 450*g* for 10 min, the total and differential cell counts of the BAL fluid were determined from the cell fraction. The supernatant was used for protein determination by Lowry's method using BSA as a standard.

Thromboxane and leukotriene assay. TxA$_2$ (measured as TxB$_2$), LTB$_4$ and LTC$_4$/D$_4$/E$_4$ in the BAL fluid were determined by using enzymeimmunoassay (EIA) kits (Amersham Pharmacia Biotech, Piscataway, New Jersey). The detection limits of the EIA assays for TxB$_2$, LTB$_4$ and LTC$_4$/D$_4$/E$_4$ were 3.6, 6 and 10 pg/ml, respectively.

Data analysis. Comparisons of data among each experimental group were carried out with analysis of variance (Scheffé test). Data are expressed as means ± s.e. *P* values less than 0.05 were considered significant.

1. American Thoracic Society. Idiopathic pulmonary fibrosis: Diagnosis and treatment; international consensus statement. *Am. J. Respir. Crit. Care Med.* 161, 646–664 (2000).
2. Wilborn, J. *et al.* Constitutive activation of 5-lipoxygenase in the lungs of patients with idiopathic pulmonary fibrosis. *J. Clin. Invest.* 97, 1827–1836 (1996).
3. Lan Tran, P. *et al.* Prevention of bleomycin-induced pulmonary fibrosis after adenovirus-mediated transfer of the bacterial bleomycin resistance gene. *J. Clin. Invest.* 99, 608–617 (1997).
4. Eitzman, D.T. *et al.* Bleomycin-induced pulmonary fibrosis in transgenic mice that either lack or overexpress the murine plasminogen activator inhibitor-1 gene. *J. Clin. Invest.* 97, 232–237 (1996).
5. Hattori, N. *et al.* Bleomycin-induced pulmonary fibrosis in fibrinogen-null mice. *J. Clin. Invest.* 106, 1341–1350 (2000).
6. Prescott, S.M., Zimmerman, G.A. & McIntyre, T.M. Platelet-activating factor. *J. Biol. Chem.* 265, 17381–17384 (1990).
7. Chao, W. & Olson, M.S. Platelet-activating factor: Receptors and signal transduction. *Biochem. J.* 292, 617–629 (1993).
8. Izumi, T. & Shimizu, T. Platelet-activating factor receptor: Gene expression and signal transduction. *Biochim. Biophys. Acta.* 1259, 317–333 (1995).
9. Honda, Z.-i. *et al.* Cloning by functional expression of platelet-activating factor receptor from guinea-pig lung. *Nature* 349, 342–346 (1991).
10. Nakamura, M. *et al.* Molecular cloning and expression of platelet-activating factor receptor from human leukocytes. *J. Biol. Chem.* 266, 20400–20405 (1991).
11. Ye, R.D., Prossnitz, E.R., Zou, A.H. & Cochrane, C.G. Characterization of a human cDNA that encodes a functional receptor for platelet activating factor. *Biochem. Biophys. Res. Commun.* 180, 105–111 (1991).
12. Kunz, D., Gerard, N.P. & Gerard, C. The human leukocyte platelet-activating factor receptor. cDNA cloning, cell surface expression & construction of a novel epitope-bearing analog. *J. Biol. Chem.* 267, 9101–9106 (1992).
13. Sugimoto, T. *et al.* Molecular cloning and characterization of the platelet-activating factor receptor gene expressed in the human heart. *Biochem. Biophys. Res. Commun.* 189, 617–624 (1992).
14. Bito, H., Honda, Z. & Shimizu, T. Cloning, expression and tissue distribution of rat platelet-activating-factor-receptor cDNA. *Eur. J. Biochem.* 221, 211–218 (1994).
15. Ishii, S. *et al.* A murine platelet-activating factor receptor gene: Cloning, chromosomal localization and up-regulation of expression by lipopolysaccharide in peritoneal resident macrophages. *Biochem. J.* 314, 671–678 (1996).
16. Ishii, S. *et al.* Bronchial hyperreactivity, increased endotoxin lethality and melanocytic tumorigenesis in transgenic mice overexpressing platelet-activating factor receptor. *EMBO J.* 16, 133–142 (1997).
17. Ishii, S. *et al.* Impaired anaphylactic responses but intact sensitivity to endotoxin in mice lacking a platelet-activating factor receptor. *J. Exp. Med.* 187, 1779–1788 (1998).
18. Leslie, C.C. Properties and regulation of cytosolic phospholipase A$_2$. *J. Biol. Chem.* 272, 16709–16712 (1997).
19. Clark, J.D. *et al.* A novel arachidonic acid-selective cytosolic PLA$_2$ contains a Ca^{2+}-dependent translocation domain with homology to PKC and GAP. *Cell* 65, 1043–1051 (1991).
20. Sharp, J.D. *et al.* Molecular cloning and expression of human Ca^{2+}-sensitive cytosolic phospholipase A$_2$. *J. Biol. Chem.* 266, 14850–14853 (1991).
21. Lin, L.L. *et al.* cPLA$_2$ is phosphorylated and activated by MAP kinase. *Cell* 72, 269–278 (1993).
22. Kramer, R.M. *et al.* p38 mitogen-activated protein kinase phosphorylates cytosolic phospholipase A$_2$ (cPLA$_2$) in thrombin-stimulated platelets. *J. Biol. Chem.* 271, 27723–27729 (1996).
23. Uozumi, N. *et al.* Roles of cytosolic phospholipase A$_2$ in allergic response and parturition. *Nature* 390, 618–622 (1997).
24. Yokomizo, T., Izumi, T., Chang, K., Takuwa, Y. & Shimizu, T. A G-protein-coupled receptor for leukotriene B$_4$ that mediates chemotaxis. *Nature* 387, 620–624 (1997).
25. Chiang, N. *et al.* Leukotriene B$_4$ receptor transgenic mice reveal novel protective roles for lipoxins and aspirin-triggered lipoxins in reperfusion. *J. Clin. Invest.* 104, 309–316 (1999).
26. Levy, B.D., Clish, C.B., Schmidt, B., Gronert, K. & Serhan, C.N. Lipid mediator class switching during acute inflammation: Signals in resolution. *Nature Immunol.* 2, 612–619 (2001).
27. Lynch, K.R. *et al.* Characterization of the human cysteinyl leukotriene CysLT$_1$ receptor. *Nature* 399, 789–793 (1999).
28. Dahlen, S.E. *et al.* Leukotrienes promote plasma leakage and leukocyte adhesion in postcapillary venules; *in vitro* effects with relevance to the acute inflammatory response. *Proc. Natl. Acad. Sci. USA.* 78, 3887–3891 (1981).
29. Nagase, T. *et al.* Acute lung injury by sepsis and acid aspiration: A key role for cytosolic phospholipase A$_2$. *Nature Immunol.* 1, 42–46 (2000).
30. Sleijfer, S. Bleomycin-induced pneumonitis. *Chest* 120, 617–624 (2001).
31. Loehrer, P.J., Johnson, D., Elson, P., Einhorn, L.H. & Trump, D. Importance of bleomycin in favorable-prognosis disseminated germ cell tumors. An Eastern Cooperative Oncology Group Trial. *J. Clin. Oncol.* 13, 470–476 (1995).
32. Scheule, R.K., Perkins, R.C., Hamilton, R. & Holian, A. Bleomycin stimulation of cytokine secretion by the human alveolar macrophage. *Am. J. Physiol.* 262, L386–L391 (1992).
33. Moseley, P.L., Hemken, C. & Hunninghake, G.W. Augmentation of fibroblast proliferation by bleomycin. *J. Clin. Invest.* 78, 1150–1154 (1986).
34. Ishii, S. & Shimizu, T. Platelet-activating factor (PAF) receptor and genetically engineered PAF receptor mutant mice. *Prog. Lipid Res.* 39, 41–82 (2000).
35. Shindou, H., Ishii, S., Uozumi, N. & Shimizu, T. Roles of cytosolic phospholipase A$_2$ and platelet-activating factor receptor in the Ca-induced biosynthesis of PAF. *Biochem. Biophys. Res. Commun.* 271, 812–817 (2000).
36. Nagase, T., Ishii, S., Shindou, H., Ouchi, Y. & Shimizu, T. Airway hyperresponsiveness in transgenic mice overexpressing platelet-activating factor receptor is mediated by an atropine-sensitive pathway. *Am. J. Respir. Crit. Care Med.* 165, 200–205 (2002).
37. Nagase, T., Aoki, T., Oka, T., Fukuchi, Y. & Ouchi, Y. ET-1-induced bronchoconstriction is mediated via ET$_B$ receptor in mice. *J. Appl. Physiol.* 83, 46–51 (1997).
38. Nagase, T. *et al.* Airway hyperresponsiveness to methacholine in mutant mice deficient in endothelin-1. *Am. J. Respir. Crit. Care Med.* 157, 560–564 (1998).
39. Nagase, T. *et al.* Airway responsiveness in transgenic mice overexpressing platelet-activating factor receptor: Roles of thromboxanes and leukotrienes. *Am. J. Respir. Crit. Care Med.* 156, 1621–1627 (1997).
40. Nagase, T. *et al.* Platelet-activating factor mediates acid-induced lung injury in genetically engineered mice. *J. Clin. Invest.* 104, 1071–1076 (1999).

Airway Hyperresponsiveness in Transgenic Mice Overexpressing Platelet Activating Factor Receptor Is Mediated by an Atropine-Sensitive Pathway

TAKAHIDE NAGASE, SATOSHI ISHII, HIDEO SHINDOU, YASUYOSHI OUCHI, and TAKAO SHIMIZU

Departments of Geriatric Medicine and Biochemistry and Molecular Biology, Graduate School of Medicine, University of Tokyo, Tokyo, Japan

Platelet activating factor (PAF) is a potent mediator potentially involved in the pathogenesis of inflammatory disorders, including bronchial asthma. Recently, transgenic mice overexpressing the PAF receptor (PAFR) gene have been established, and exhibit bronchial hyperresponsiveness, one of the cardinal features of asthma. To elucidate the molecular and pathophysiologic mechanisms underlying PAF-associated bronchial hyperreactivity, we studied airway responsiveness to methacholine (MCh) and serotonin (5-hydroxytryptamine; 5-HT) in PAFR-transgenic mice. In addition, we examined the role of the muscarinic receptor in PAF-induced responses and the binding activities of the muscarinic receptor. The PAFR-transgenic mice exhibited hyperresponsiveness to MCh and PAF; however, no significant differences in 5-HT responsiveness were observed between the control and PAFR-transgenic mice. The administration of atropine significantly blocked PAF-induced responses in PAFR-transgenic mice. There were no differences between the two phenotypes in the binding activities of muscarinic receptor. Morphometric analyses demonstrated that PAFR overexpression did not affect airway structure. These findings suggest that the muscarinic pathway may have a key role in airway hyperresponsiveness associated with PAFR gene overexpression. More generally, PAFR-transgenic mice may provide appropriate models for study of the molecular mechanisms underlying PAF-associated diseases.

Keywords: platelet activating factor; asthma; airway hyperresponsiveness; transgenic mouse

Platelet activating factor (PAF) is a proinflammatory phospholipid mediator that has various potent properties (1–4). PAF mediates its biologic effects via activation of a G-protein–coupled, seven transmembrane receptor (1, 3–5). Complementary DNAs (cDNAs) and genes for the PAF receptor (PAFR) have been cloned from various species, including guinea pigs and humans (5–11). To examine the pathophysiologic role of PAF *in vivo*, we have established transgenic mice ubiquitously overexpressing PAF receptor (12). Recently, we also established a mutant mouse lacking PAFR, and demonstrated that PAF could be involved in anaphylactic responses (13).

It has been indicated that PAF plays a substantial role in the pathogenesis of bronchial asthma (14, 15). Moreover, it has been demonstrated that the level of expression of PAFR messenger RNA (mRNA) in the lung is increased in humans with asthma (16). In asthmatic children, deficiency of plasma PAF acetylhydrolase is associated with respiratory dysfunc-

tion (17, 18), and in a mouse model of asthma, recombinant PAF acetylhydrolase inhibits airway inflammation and hyperreactivity (19). Bronchial hyperreactivity, which is a major characteristic of asthma, is augmented by the administration of exogenous PAF (20). However, the exact pathophysiologic roles of PAF in the pathogenesis of bronchial asthma remain to be elucidated.

In the current study, we investigated the pathophysiologic mechanisms underlying PAF-associated airway hyperresponsiveness (AHR). We studied the airway responsiveness of PAFR-transgenic mice to methacholine (MCh) and serotonin (5-hydroxytryptamine; 5-HT). We then examined the involvement of the muscarinic pathway in PAF-induced responses, and performed binding assays for muscarinic receptor. We further assessed airway structure, including smooth muscle, using morphometry.

METHODS

Mice

PAFR-transgenic mice were established as previously described (12). Mutant mice and their littermate controls were used in this study.

Animal Preparation

Animals were anesthetized with pentobarbital sodium (25 mg/kg, intraperitoneally) and ketamine hydrochloride (25 mg/kg, intraperitoneally) in combination, and were mechanically ventilated with tidal volumes of 10 ml/kg, respiratory frequencies of 2.5 Hz and a positive end-expiratory pressure of 2 cm H_2O. The thorax was widely opened by means of a midline sternotomy, but the vagus nerve was not sectioned. Lung resistance (R_L) and elastance (E_L) were measured as previously described (21–23).

Airway Responsiveness to 5-HT or MCh

Following baseline measurement, each dose of 5-HT aerosol (0.15 to 10 mg/ml) or MCh aerosol (0.63 to 80 mg/ml) was administered for 1 min in a dose–response manner. As previously reported (22, 23), airway responsiveness to 5-HT or MCh was assessed from the concentration of agonists required to increase R_L to 200% of baseline values (EC_{200} R_L).

Airway Responsiveness to PAF

Following baseline measurement, each dose of PAF (5 to 20 μg/kg) was administered intravenously and measurements were made.

Effects of Atropine on PAF-Induced Responses

Two minutes before receiving the intravenous bolus of 10 μg/kg PAF, mice were intraperitoneally pretreated with either saline or 10 μmol/kg atropine sulfate. After baseline measurements, PAF was administered via the jugular vein and measurements were made.

Binding Assays for Muscarinic Receptor

From each mouse preparation, five or six whole lungs were obtained and homogenized together in a ×10 volume of binding buffer (25 mM 4-(2-hydroxyethyl)-1-piperazine-N'-2-ethanesulfonic acid [pH 7.4], 0.25 M sucrose, 10 mM $MgCl_2$) containing a proteinase inhibitor cocktail (Complete; Roche, Mannheim, Germany) and 20 μM amidino phenyl methyl sulfonyl fluoride (Sigma, St. Louis, MO). After centrifugation (800 × *g*

for 20 min at 4° C), the supernatants were further centrifuged at 123,000 × g for 1 h. The pellets were mashed once and recentrifuged at 140,000 × g for 1 h. The final pellets were resuspended in the same buffer. The binding assays were done in duplicate in the absence or presence of 50 nM PAF. The reaction mixture consisted of 150 μl of the binding buffer containing [N-methyl-^{3}H]scopolamine (2.51 TBq/mmol), a nonselective muscarinic antagonist, at increasing concentrations of 0.0625 to 2 nM, and 50 μl of the membrane protein (95 μg). The mixtures were incubated in a 96-well microplate at 25° C for 1.5 h, followed by filtration and washing as described previously (24). The radioactivities of dried filters were determined as reported (24). Nonspecific binding was defined as the binding measured in the presence of 20 μM methacholine.

Binding Assays for PAFR

The lung membrane was obtained as described previously. Binding assays for PAFR were performed in the same manner as previously described, with [^{3}H]-WEB2086, a PAFR-selective antagonist, at increasing concentrations at 3.13 to 100 nM (703 GBq/mmol). Nonspecific binding was defined as the binding in the presence of 50 μM cold WEB2086.

Morphometric Study

In four animals from each group, we quantitated airway smooth muscle and lamina propria, using morphometric techniques as previously reported (25, 26).

Data Analysis

Comparisons of physiologic and morphometric data among the experimental groups were done through analysis of variance (Scheffe's test) or Student's t test. Data are expressed as mean ± SE. Values of p < 0.05 were taken as significant.

RESULTS

Airway Responsiveness to 5-HT or MCh Administration

The control and PAFR-transgenic mice showed no significant differences in baseline E_L and R_L. Figure 1 shows 5-HT dose–response curves for E_L in the two groups. There was no difference in elastic responses to 5-HT. MCh dose–response curves for E_L are shown in Figure 2. Responses in the PAFR-transgenic mice were significantly greater than in the control group at MCh doses of > 2.5 mg/ml.

Responses for R_L are summarized in Figure 3. As shown, there were no differences between the two groups in 5-HT responsiveness. However, airway responsiveness to MCh in PAFR-transgenic mice was significantly greater than in control mice ($logEC_{200}$ R_L = 0.950 ± 0.076 versus 1.462 ± 0.039, p < 0.001).

Airway Responsiveness to PAF

Following the administration of 20 μg/kg PAF to five PAFR-transgenic mice, two animals died immediately from cardiac arrest, whereas no animals died in the other groups. Responses for E_L and R_L are shown in Figure 4. After administration of each dose of PAF (5 to 20 μg/kg), significant differ-

Figure 2. MCh dose–response curves for E_L in control and PAFR-transgenic mice (n = 7 for each group). *p < 0.01 compared with control mice. BAS = baseline; SAL = saline. -O- Control; -●- Transgenic.

ences in pulmonary responses were observed between the control and PAFR-transgenic mice, and the effects of PAF were enhanced at higher doses in the PAFR-transgenic group.

Effects of Atropine on PAF-Induced Pulmonary Responses

Effects of atropine on PAF-induced pulmonary responses are demonstrated in Figure 5. As shown, the control mice exhibited no responses to 10 μg/kg PAF after either saline or atropine pretreatment. In the PAFR-transgenic mice pretreated with saline, PAF administration induced increases in R_L and E_L. Pretreatment with atropine significantly inhibited PAF-induced responses in the PAFR-transgenic mice.

Binding Assays for Muscarinic Receptor and PAFR

Results of binding assays for muscarinic receptor are summarized in Table 1. In either the absence or presence of PAF, there were no differences between the control and PAFR-transgenic mice in dissociation constant (Kd) or binding maximum (Bmax) values for [N-methyl-^{3}H]scopolamine, a nonselective muscarinic antagonist, suggesting that the binding activities for muscarinic receptors in the PAFR-transgenic lungs were similar to those in the controls.

As shown in Figure 6, the binding activities for PAFR in the PAFR-transgenic lungs were markedly greater than in the control lungs.

Morphometric Study

Table 2 summarizes the morphometric data for airway size and roundness. There were no significant differences between the PAFR and control mice in number of airways, airway size, or airway roundness, indicating that there were no significant biases between the experimental groups in terms of airway selection.

As shown in Figure 7, there were no significant differences between the PAFR and control groups in thickness of the lamina propria or airway smooth muscle. In addition, no significant difference in inner wall area was observed between the
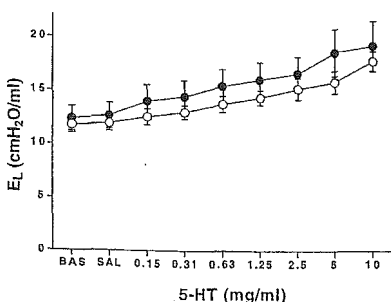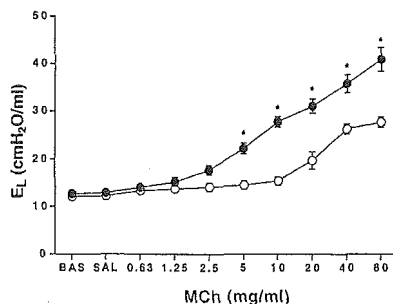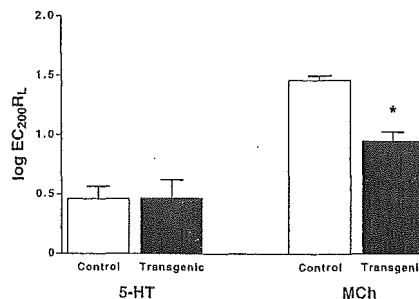

Figure 1. Serotonin (5-HT) dose–response curves for E_L in control and PAFR-transgenic mice (n = 4 for each group). BAS = baseline; SAL = saline. -O- Control; -●- Transgenic.

Figure 3. Airway responsiveness expressed as the concentration of agonists required to double lung resistance (EC_{200} R_L). *p < 0.001 compared with control mice. 5-HT = serotonin; MCh = methacholine.